MODELING ELECTRICAL ENERGY PRODUCTION IN NORTHWESTERN CYPRUS BASED ON SOLAR AND WIND MEASUREMENTS

A THESIS SUBMITTED TO THE BOARD OF CAMPUS GRADUATE PROGRAMS
OF MIDDLE EAST TECHNICAL UNIVERSITY NORTHERN CYPRUS CAMPUS

BY

MEHMET YENEN

IN PARTIAL FULLFILLMENT OF THE REQUIREMENTS

FOR

THE DEGREE OF MASTER OF SCIENCE

IN

SUSTAINABLE ENVIRONMENT AND ENERGY SYSTEMS

JANUARY 2015

Approval of the Board of Graduate Programs _____

Prof. Dr. M. Tanju MEHMETOĞLU

Chairperson

I certify that this thesis satisfies all the requirements as a thesis for the degree of Master of Science _____

Assoc. Prof. Dr. Ali MUHTAROĞLU

Program Coordinator

This is to certify that we have read this thesis and that in our opinion it is fully adequate, in scope and quality, as a thesis for the degree of Master of Science.

_____

Assist. Prof. Dr. Murat FAHRİOĞLU

Supervisor

Examining Committee Members

Assoc. Prof. Dr. Ali Muhtaroğlu	Electrical and Electronics Engineering Dept. METU NCC	_____
Asst. Prof. Dr. Murat Fahrioğlu	Electrical and Electronics Engineering Dept. METU NCC	_____
Assoc. Prof. Dr. Derek Baker	Mechanical Engineering Dept. METU	_____
Assoc. Prof. Dr. Eray Uzgören	Mechanical Engineering Dept METU NCC	_____
Assoc. Prof. Dr. Serkan Abbasoğlu	Energy Systems Engineering Dept. CIU	_____

I hereby declare that all information in this document has been obtained and presented in accordance with academic rules and ethical conduct. I also declare that, as required by these rules and conduct, I have fully cited and referenced all material and results that are not original to this work.

Name, Last name : Mehmet Yenen

Signature :

ABSTRACT

MODELING ELECTRICAL ENERGY PRODUCTION IN NORTHWESTERN CYPRUS BASED ON SOLAR AND WIND MEASUREMENTS

Mehmet Yenen

Supervisor: Assist. Prof. Dr. Murat Fahrioğlu

January 2015, 78 Pages

This thesis presents the solar and wind energy assessment and aims to model the link between measurement and electrical energy production from wind and solar resources in Northwestern Cyprus. The measurement systems were installed and the measurements from these systems were analyzed thoroughly to meet the expectations of this thesis. Existing mathematical models were used to calculate electrical energy production figures for wind and solar energy. A circuit based Photovoltaic (PV) model from the literature was used and compared with Serhatköy PV module spec sheet parameters. In order to validate the model, Serhatköy PV farm Global Tilted Irradiation (GTI) data was used and electricity generation estimation there was obtained with an annual average of 5% error. Using Global Horizontal Irradiation (GHI) and Direct Normal Irradiation (DNI) measurements of Middle East Technical University Northern Cyprus Campus (METU NCC), a prediction method in the literature was used to estimate the GTI on Serhatköy. Using the methodology developed in this thesis, these gaps in energy production are filled, and a better potential estimate can be obtained. One of the main goals of this thesis is to verify the developed methodology to be able to predict PV electricity production with reasonable accuracy for any specific location in Northwestern Cyprus. A mathematical model from the literature was used for wind energy generation. Solar electricity generation estimation indicated an annual 2118 kWh/m^2 GTI in Serhatköy, with an annual average error of 2.37%. Using estimated GTI value from METU NCC measurement station, Serhatköy electricity generation was predicted with an annual average error of about 4%. Wind energy electricity generation prediction was below world standards unlike the results of solar energy assessment. Numerical comparisons were shown in this thesis and compared to other results with European countries. Although a methodology was developed to estimate the wind electricity generation, it is concluded that it can be only applied to METU NCC.

Keywords: METU NCC, Solar Energy, Wind Energy, Electrical Energy Conversion

ÖZ

KIBRISIN KUZEYBATISINDA RÜZGAR HIZI VE GÜNEŞ RADYASYONU ÖLÇÜMLERİNE DAYALI ELEKTRİKSEL ENERJİ ÜRETİMİ

Mehmet Yenen

Yüksek Lisans, Sürdürülebilir Çevre ve Enerji Sistemleri Programı

Tez Yöneticisi: Yrd. Doç. Dr. Murat Fahrioğlu

Ocak 2015, 78 Sayfa

Bu tez, güneş ve rüzgâr enerjilerinin değerlendirmesini sunmaktadır ve Kıbrıs'ın kuzeybatısında rüzgâr ile güneş enerjilerinin ölçüm ve elektrik enerji üretimi arasındaki bağı modellemeyi amaçlamaktadır. İlgili bilgiyi toplamak için ölçüm sistemleri kurulmuş ve bu sistemlerden elde edilen bilgiler bu tezdeki beklentilerin karşılanması için ayrıntılı bir biçimde analiz edilmiştir. Bu bilgiler, hâlihazırdaki matematiksel modeller kullanılarak rüzgâr ve güneş enerjisinden üretilebilir elektrik enerjisi figürleri hesaplanmıştır. Literatürdeki bir devre temelli Fotovoltaik (PV) modeli kullanılmış ve Serhatköy PV parça özellik parametreleri ile karşılaştırılmıştır. Bu modeli tasdik etmek amacıyla Serhatköy PV merkezi GTI bilgisi kullanılmış ve elektrik üretim bilgisi yıllık ortalama %5 hata payıyla elde edilmiştir. Ortadoğu Teknik Üniversitesi Kuzey Kıbrıs Kampüsü'ndeki (ODTU KKK) GHI ve DNI bilgileri, literatürdeki bir tahmin metodolojisini kullanarak Serhatköy'deki GTI bilgileri yakınsanmıştır. Bu tezde geliştirilen yöntem ile enerji üretimindeki bu boşluklar doldurulmuş ve daha kaliteli bir tahmin elde edilmiştir. Bu tezin asıl amaçlarından birisi, geliştirilen yöntemin Kıbrıs'ın kuzeybatısında herhangi bir alanın spesifik ölçümlerini makul doğrulukla yakınsayabileceğini onaylamaktır. Rüzgâr elektrik üretimi içinse literatürde hâlihazırdaki bir model kullanılmıştır. Serhatköy'deki tahminsel sonuç yıllık ortalama %2.37 hata payı ile yıllık 2218 kWh/m^2 bulunmuştur. ODTÜ KKK'daki tahminsel GTI değeri kullanılarak, Serhatköy elektrik üretimi %4'lük bir hata payı ile belirlenmiştir. Rüzgâr bazlı elektrik üretim ölçümleri ise güneş enerjisini ölçümlerinin aksine dünya standartlarının altında sonuçlanmıştır. Numerik karşılaştırmalar tezde sunulmuş ve diğer Avrupa ülkelerindeki sonuçlar ile karşılaştırılmıştır. Rüzgâr enerjisi için bir yöntem geliştirildiğine karşılık bu yöntemin sadece ODTÜ KKK'da uygulanabilirliğiyle sonuçlanmıştır.

Anahtar Kelimeler: ODU KKK, Güneş Enerjisi, Rüzgar Enerjsi, Elektriksel Enerji dönüşümü

DEDICATION

To my beloved Family

For their unconditional support, trust and encouragement.

ACKNOWLEDGEMENTS

First and foremost I offer my genuine gratitude to my supervisor, Dr. Murat Fahrioglu, who has supported and guided me throughout the completion of my thesis with his patience, skill and knowledge whilst providing me the explore the problem statement in my own way. It was due to his support, timely feedback and perceptive comments that I was able to complete my thesis. I thank him whole-heartedly and attribute the level of my Master's degree to his advice, encouragement and efforts.

Besides my advisor, I would like to thank the other members of my thesis committee, for providing me kind support, confidence and the necessary data to successfully complete the thesis.

I would like to thank Mr. Arsalan Tariq for providing me the electricity and solar irradiation data at Serhatköy and Mr. Furkan Ercan and Mr. İzzet Akmen for their technical support and encouragement.

I would like to thank my friends who helped me during my work. The technical assistance, I would also like to acknowledge and thank Moslem Yousefzadeh, Eda Köksal, İpek Alemdar, Didem Gürdür, Syed Zaid Hasany, Muhammad Azhar Ali Khan, Fassahat Ullah Qureshi, Kumudu Gamage, Rayaan Harb, Sajed Sadati, Musa Hadera, Onur Erensoy, Cem Demirsoy, Fatih Şener, Mertcan Çeki, Zuhal Topaloğlu and many others for the friendly environment.

Last but not the least; I would like to express my love, affection and gratitude to my wife, Rahime Yenen, and my little son, Yusuf Ali Yenen, and my other family members in general for their continuous love, prayers and staunch support. This work would have been beyond possible if not for them.

TABLE OF CONTENT

LIST OF TABLES

LIST OF FIGURES

NOMECLATURE

GaAs: Gallium Arsenide

a-Si: Amorphous-Silicon

CdTe: Cadmium Telluride

CIS: Copper indium dieseline

Eg: Band gap energy of the semiconductor (eV)

Eg0: Band gap energy at T=0K (eV)

I: Cell output current (A)

I_0: Dark saturation current (the diode leakage current density in the absence of light) (A)

I_d: Diode current (A)

I_{MP}: Current at the maximum-power point (A)

$I_{0,r}$: Cell‘s short circuit current at STC (A)

I_{PH}: Light-generated current or photocurrent (A)

I_{SC}: Short-circuit current (A)

I_{SCR}: Short circuit current at reference temperature (A)

I_{SH}: Current through the shunt resistance (A)

k: Boltzmann‘s constant (1.38 × 10-23 J/K)

k_i: Cell‘s short-circuit current temperature coefficient (A/K)

n: Ideality factor (a number between 1 and 2 that typically increases as the current decreases)

Np: number of cells connected in parallel

Ns: number of cells connected in series

P: Power (W)

P_{MP}: Power at the maximum-power point (W)

PV: Photovoltaic

q: Electron charge (1.602×10^{-19} C)

Rs,final: Final value of Rs (Ω)

Rs: Series resistance of cell (Ω)

Rsh: Shunt resistance of cell (Ω)

S: Solar irradiance (W/m^2)

Si : Silicon

Si-mono: Monocristalline-Silicon

Si-poly: Polycrystalline-Silicon

Sr : Reference solar radiation (1000 W/m^2)

STC: Standard Test Condition (AM=1.5; T=25C; S=1000

W/m^2)

T: Cell working temperature (K)

T_r: Cell‘s reference temperature in degree K

Tr1: Cell‘s reference temperature in degree Fahrenheit (40)

V: Cell output voltage (Volt)

V_d: Diode voltage (Volt)

V_{mp}: Voltage at the maximum-power point (Volt)

V_{OC}: Open-circuit voltage (Volt)

V_t: Thermal junction voltage (mV)

α, β: Parameters which define Band gap energy of the semiconductor (eV/K^2, K)

ρ: density of the air (kg/m^3)

V: Velocity of the air (m/s)

A: Span Area of the turbine (m^2)

P: Output power (W)

Cp: Power Coefficient

ρ: density of air (kg/m3)

P: air pressure (Pa)

R: specific gas constant = 287.058 J/(kg.K)

T: absolute temperature (K)

CHAPTER

1. INTRODUCTION

1.1. Motivation

Understanding the global energy problems and its influence on the environment, rapid depletion of fossil fuel resources brings about the need to look for alternative energy resources in order to find out a solution for future energy generation. Strategically positioned in central Europe and the Middle East, Cyprus has a significant potential of energy harvesting. Nevertheless in Cyprus, like on many islands, which does not have connection to a large electricity network, electrical energy generation entirely depends on imported energy sources such as oil. One of the possible reasons is the energy generation capacity of solar and wind energy systems are not known well in the island of Cyprus. Although there are several publications regarding the solar potential of the island, there is very little academic study on conversion of solar potential to electrical energy.

Middle East Technical University Northern Cyprus Campus (METU NCC) is a university located in Northwestern part of Cyprus. Several years ago, our research group at METU NCC installed solar and wind measurement stations to investigate the energy capacity of Northwestern Cyprus where the campus is located. The primary motivation for this thesis is to develop a methodology for modeling the link between measurement and electrical energy production. In case of solar energy, there exists a photovoltaic (PV) power station (Serhatköy PV farm) located about 5 km from campus. Hence an existing model [**1**] has been applied to this PV power station to predict electrical energy production using irradiation measurements from our campus and using measurements from Serhatköy PV farm. This helped validate the PV model used and gave us a tool to predict electrical energy production using irradiation measurements. Similar methodology was used for wind energy systems to predict electrical energy production [**2**] using measurements from our campus. However since there is no nearby wind farm the results were compared to a wind farms further away from campus in Paphos and Larnaca for validation. The proposed methodology was then applied using METU NCC measurements to calculate capacity factors for both wind and solar energy production in this region. These capacity factors were then compared

with capacity factors from different parts of Europe in order to assess the solar and wind energy situation in Northwestern Cyprus.

1.2. World Energy Status

Electricity generation, as one of the main types of energy, faces a challenge due to the fact that the main source of electricity generation is fossil fuels and they are about to diminish. This is one of the motivations to base this thesis on solar and wind energy system. Moreover, increasing greenhouse gases emission causes global warming. Cyprus has good solar resources but the wind energy capacity is not known well. As a Mediterranean island, solar power is expected to be more promising than wind potential. However, the energy generation capacity of solar and wind energy systems are not considered in the Northwestern part of the island. METU NCC solar and wind energy measurement stations were used in order to link the measured data and electrical energy generation. To note before starting with the analysis, it is worthy to qualify and quantify the energy situations in the world.

An annual report [**3**] about energy situation of the world including 2013 results indicates that world energy generation and consumption is increasing day by day. There are several factors, which may cause the increasing energy generation; growing population, economic growth and also technological level up are some of them. Statistical review of electricity generation by regions is illustrated in Figure 1. Figure 1 indicates that annual total energy generation is increasing dramatically by a decade.

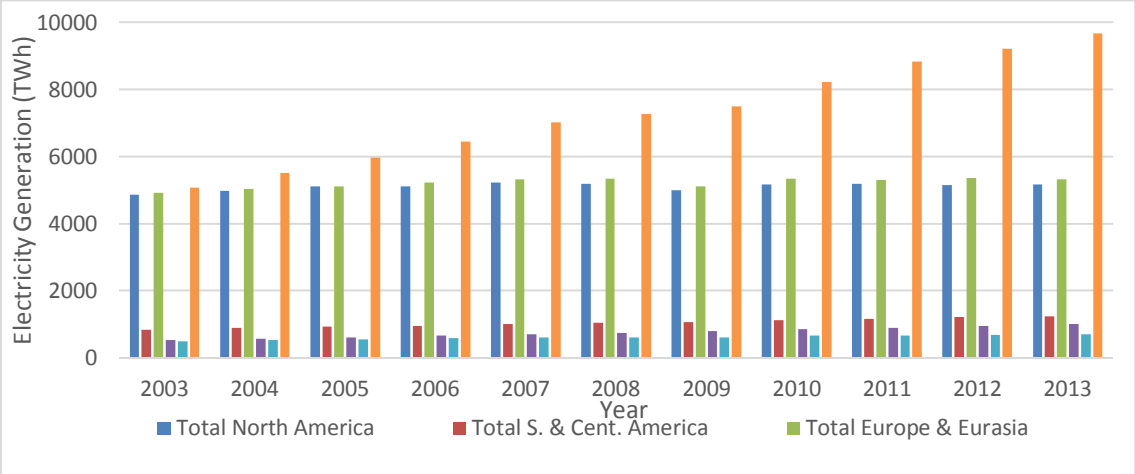

*Figure 1. Statistical review of electricity generation (TWh) [**3**]*

Asia pacific is becoming more attractive in the energy area due to the excessive need for energy. For example, China is the leading country in terms of electricity generation. An extensive study [**4**] that has been carried out to analyze socio-economics of electricity generation in China demonstrates that there are six different fields of energy generation. Nuclear energy, hydroelectricity, renewables, oil, coal and natural gas are the primary fields and the percentage of usage is 5, 6, 2, 33, 24 and 30 respectively. However, China generates 70 % of its electricity from coal. On the other hand, there is a significant decrease in energy intensity in European Union [**5**] due to the fact that renewable energy use is growing faster. The study indicated that currently 19.9 % of the electricity generation comes from renewable energies. Hydropower has the largest share among other renewable types (11.6%), followed by wind (4.2%), biomass (3.5%) and solar (0.4%). For instance, 98 % of the electricity generation of Albania comes from hydro power or Turkey has 31 % electricity production from hydropower [**6**]. According to Table 1 [**7**], the total electricity generation is obtained from renewables in the world.

Table 1. Total electricity generation from renewable in the world in 2011 [7].

Type of Renewable	Energy Generation MWh
Bioenergy	424
Hydro	3490
Wind	434
Geothermal	69
Solar PV	61
Concentrating Solar	2
Marine	1
Total	4481

Another annual report [**7**], World Energy Outlook 2013, has carried out that hydro power is the largest numerator, which consists of 78 % of the total renewable energy generation. Other than the hydro power, wind energy installation is promising. Due to the tertiary effect of wind speed to the power generation, the wind energy is an attractive solution to the world's increasing energy demand [**2**]. However, wind energy power output is not stable like it is in the hydro power plants due to highly stochastic wind velocity [**8**], [**9**], [**10**], [**11**]. Solar energy is more predictable if there is enough measured data [**12**] [**13**]. One comprehensive study that has been carried out to review the wind potential of the world, emphasizes that global wind power potential was 72 TW in the year 2000 [**14**]. It also indicates estimated wind power potential is enough to produce five times global energy demand.

1.3. Solar and Wind Energy Status of European Region Countries

Some of the European region countries solar and wind energy status are presented.

1.3.1. Portugal

A well-rounded study covers the benefits of developing PV generation market in Portugal, and current PV status of Portuguese PV electricity sector is presented [**15**]. According to the authors, renewable energy sources have a priority access for the energy generation. Moreover, the EU directive 2009/28/EC target for Portugal is 31% of energy from renewable energy in 2020 [**16**]. There is a dramatic increase in installed PV capacity of

Portugal. In 2013, the installed capacity of solar PV system is 277.9 MW_p and the electricity generation is 437 GWh [**17**]; therefore, the capacity factor of the system is 17.95%. On the other hand, the wind energy capacity reaches 4709 MW installed capacity, which is 23% of the renewables [**18**]. Considering the amount of wind capacity, 11.9 TWh of electricity was supplied to the electricity grid in 2013; therefore, the wind energy capacity factor is calculated as 28.84%.

1.3.2. Germany

Solar and wind energy plays significant role in German electricity system in terms of increasing installed capacity. In 2011, for instance, the installed capacity of wind, biomass, hydro and solar are 29, 7, 4, 25 GW respectively [**19**]. According to an article [**15**], Germany is the leader in photovoltaic energy. Accordingly, the author emphasizes the legal instruments in the promotion of electricity from renewable source is Renewable Energy Source Act and its amendments. To note some of the information about this law, it regulates the connection of the renewable energy installations to the grid and provides energy purchasing and transmission; in other words, it also sets feed-in-tariffs. Moreover, Net-metering is another option in Germany with various tariffs. Accordingly, in addition of renewables to the grid, Germany aims to reduce Carbone-Dioxide (CO_2) output by 80% for the year 2050 in comparison with the year 1990 [**20**]. Another extensive study [**21**] illustrates 35% of renewable energy share reduces 40% emission by 2020. As a result, Germany had 36337 MW installed PV capacity (this is approximately 50% of European Union countries) in 2013 and about 31 TWh electricity was generated from only PV, thus the capacity factor is calculated as 9.73%. On the other hand, total installed wind capacity was approximately 34660 MW on land and 903 MW offshore in 2013 (this is almost 29 percent of European Union countries). 53.4 TWh electricity was generated from wind turbines [**18**]; so capacity factor of wind is calculated as 17.09%.

1.3.3. France

Presently France heavily depends on nuclear energy; most of the electricity generation comes from Nuclear power; yet, renewable energy shares 13% only [**15**]. Moreover, like in Germany, French renewable energy sources support feed-in-tariffs. Cumulative PV capacity reached 4.7 GW in 2013. The wind energy installation was 8254

MW at the end of 2013 [**22**]. In comparison with Germany, France renewable percentage of electricity generation is low.

1.3.4. Greece

Greece was the first European country to build a wind farm and one of the first to apply a PV plant [**23**]. According to the authors, Greek Government also provides feed-in-tariff scheme; therefore, 7947 licenses have been submitted in less than 2 years' time. However, Greek energy system is one of the most carbon intensive energy systems in Europe [**24**]. In addition, Lignite is the primary energy source and is used in electricity generation exclusively. As a member of European Union, Greece has to achieve European Energy Policy about renewable energy system integration; such as 20% of the energy consumption comes from renewable sources by 2020. Nevertheless, the cumulative installed RES power has not increased as expected level [**15**]. One of the possible reason is the financial crisis in 2008. Due to the effect of crisis, renewable energy producers have been given extra taxes. In consequence, the total installed PV and wind capacity reached 2419 and 1865 MW respectively in 2013.

1.3.5. United Kingdom

Although it is one of the European Union countries, British PV market is growing slowly up to the introduction of PV feed-in-tariff in 2010. Therefore, solar power usage has increased rapidly in recent years. Nevertheless, the UK has significant potential on wind energy; that is, approximately 40% of Europe's entire wind resource [**18**]. Moreover, a comprehensive study [**25**] pointed out a development for grid connection of North and Baltic Seas cause the installed wind capacity to increase. Currently, it has 10531 MW installed wind capacity at the end of 2013.

1.3.6. Spain

Among the other European Union countries, Spain offers very attractive conditions for development of PV energy due to high solar radiation intensity. Until 2008, there had been a high investment for utilization of PV system; yet, the market collapsed due to the financial crisis in Europe in 2008. According to an article [**15**], only 99 MW power were installed. Spain is the second biggest PV capacity after Germany in Europe. Apart from

these, Spain is the second in terms of installed capacity. It is done because the regulations in Spain guaranteed feed-in-tariff valid for 25 years [**15**]. On the other hand, wind energy share has a worthy place; 22959 MW installed capacity of wind energy supply the electricity grid [**18**] in 2013. Moreover, 54.3 TWh of electricity is generated, and so the capacity factor of wind energy is 26.99% which is promising.

1.3.7. Cyprus

A comprehensive study [**26**] has been carried out to examine the options of using renewable energy sources in the power system in order to reduce the air pollutants. The authors defined capacity targets by renewable energy system technology and estimated the electricity production. Note that the targets are set by the government of Republic of Cyprus. The capacity target results are presented in Table 2. Wind power experienced a dramatic increase such that global installed capacity at the end of 2011 is around 238 GW. Furthermore, Southern Cyprus has made an important attempt to reach European Union's renewable energy target by 2020 [**27**]. The state-owned Electricity Authority of Cyprus has to buy 113.5 MW of energy from two new operators, Orites wind farm in Paphos and Ketonis wind farm in Larnaca [**28**].

*Table 2: Capacity target by Renewable Energy System technology and estimated electricity generation in Cyprus [**26**]*

RES Technology	Capacity Target MW	Capacity Factor	Electricity Production GWh/year
Wind Power	165	25%	361.35
Solar Thermal	25	65%	142.35
PV system	14	30%	36.79
Biomass	4	75%	26.28
Biogas	3	75%	20.71
Total	211		

The energy situation and renewable energy portfolio in the world is summarized. In Cyprus region, solar and wind profiles are also going to be indicated, analyzed, and demonstrated. To begin with, the installed power stations in the Northern part of the island can be illustrated in Table 3. The total installed capacity is 338.27 MW; nonetheless, the Dikmen gas turbine has not been used for several years due to less power conversion

efficiency. Therefore, it can be explained that the actual usable installed capacity is 318.27 MW. The two steam turbines in the Teknecik Power Plant provide electricity to the base load of the system supported by six other diesel generators. The only renewable system on the northern part of the island is Serhatköy Photovoltaic Power plant which has the capacity of 1.27 MW. To note one of the significant aspects of this analysis, more than 99 % of the electricity generation in Northern Cyprus comes from Fuel oil No: 6, which is one of the most harmful substances in terms of CO_2 production [**2**]. Nonetheless, meteorological data indicate that Mediterranean islands tend to have a good solar resource [**29**], and Cyprus is the third great island in terms of size. For instance, Malta is a small island in Mediterranean. An extensive study indicates that the daily average solar irradiation is 5.29 kWh/m^2 and a total annual solar irradiation is 1933 kWh/m^2 [**30**], yet there is not enough usable land area.

*Table 3: Kıb-Tek power stations, capacities and status [**31**]*

Power Stations	Definition	Capacity (MW)	%	Status
Teknecik	2 x 60 MW Steam Turbine	120.00	35.47%	Active
Teknecik	6 x 17.5 MW Diesel Generator	105.00	31.04%	Active
Kalecik	92 MW Diesel Generator	92.00	27.20%	Active
Serhatköy	1.27 MW Photovoltaic	1.27	0.38%	Active
Dikmen	20 MW Gas Turbine	20.00	5.91%	Not Active
	Total	**338.27**		

1.4. Solar and Wind Energy Measurements and Uncertainties for Measured data

While measuring solar and wind data at METU NCC, it was realized that some points of the datasets did not look correct. Details were discussed in Section 2.2.1, 2.2.2, 3.2.2 and 3.2.3. For instance, some periods of the wind data measurement station, 40th meter anemometer did not measure the wind speed due to technical problems. Moreover, from April 2014 till May 2014 solar resources indicated very low, and thus it did not seem correct. In addition to that, some periods of temperature measurements yielded incorrect datum. Due to the realized uncertainties in solar and wind energy dataset, control check of the dataset was necessary.

1.5. Objectives of the Thesis

As mentioned earlier regarding lack of information about solar and wind energy resources and the link between measurements and electricity generation in Northwestern Cyprus, this thesis is a summary of how much electricity can be generated using presented methodology. Contributing on filling of this the gap about solar and wind energy in the island of Cyprus can be a solution for future energy problems. This supports the motivation to develop a methodology for modeling the link between measurement and electricity generation.

In this context, the overall aim of the thesis is to analyze and quantify the measurements of solar and wind energy, and also to find the link between energy productions of solar photovoltaic system and wind energy system for specifically the location of Northwestern Cyprus. The analysis described in this thesis focuses the impact of PV and wind energy on:

- Mathematical modeling of solar/wind based on equation found in the literature,
- Validating the models with using Serhatköy solar data, and comparing wind energy results with Southern Cyprus wind farm
- Finding the link between measured data and electrical energy production,
- Numerical evaluation and comparison of the capacity factors for both solar and wind energy systems with other regions of the world.

1.6. Scope of the Thesis

Based on the lack of information about solar and wind energy for Northwestern Cyprus and the certain gaps in the literature mentioned in the study, the objective for this study is to develop a clear methodology to quantify solar and wind energy conversion potential in Northwestern Cyprus. Application of the methodology uncovers the electricity generation of solar PV and wind energy status, and thus it reveals where Cyprus potential electricity generation capacity from presented renewables is situated compared with other European countries. The main goal of this study is estimating electricity generation of

Serhatköy PV plant using METU NCC measurements; with this type of tool METU NCC measurements can predict PV plant production with reasonable accuracy.

For solar energy part, only photovoltaic systems are discussed in the scope of the thesis. Thermal analysis of solar energy is out of scope of the thesis. Solar measured data was analyzed through the PV part using an already existing circuit based mathematical model. The study indicates why single diode model has been used instead of two diode model.

A control check of measured solar data and PV model is necessary due to the presented uncertainties in the dataset. In addition to this, model validation would clear the minds although the model is an existing model in the literature. For dataset control and model validation Serhatköy solar PV power plant irradiation and electricity generation data was added in the scope of the thesis.

On the other hand, wind data set was only compared with each other due to the fact that there is not any available wind data for the location of Northwestern Cyprus. Moreover, the wind is a viable energy, geographical properties affect the variation of the data. There are four measurement devices with different heights of the tower so that it is possible to control data itself and correlation in the heights were added in the scope of this study. Energy generation model was taken from the literature and other research was also used. As mentioned earlier, there is not any power plant for that specific location in order to validate the energy generation model. Since the model was used in the literature, it is regarded as not necessary to validate the model.

Application of the methodology reveals the facts about solar and wind energy generation for Northwestern part of the island. The next step is to observe the energy generation capacity status of the island. Lastly, numerical comparison of both solar and wind energy electricity generations with different parts of the world are added in the scope of this work.

2. METHODOLOGY FOR SOLAR ENERGY

2.1. Campus Solar Measurement System

In this part of thesis, solar data collecting systems currently used in METU NCC were focused on. There are three types of solar data, global solar radiation, beam (direct) solar radiation (reflected) and diffuse solar radiation. In order to measure these kinds of solar radiations, solar measuring station was constructed. This station includes a pyrometer and a pyrheliometer which are connected to Solys 2 sun tracker.

A pyrometer is designed in order to measure global solar radiation and diffuse solar radiation. Pyrometer is an instrument that converts sun fluxes into electrical signal which results in radiant flux $^{W}/_{m^2}$. To achieve the required spectral and directional characteristic pyrometer uses thermopile detectors and glass domes. An optimal setting for the data interval is to sample and store one minute averages. Combination with data logger provides the storage of average ten minutes data. A tilted solar radiation can be collected using pyrometer for specific angles. The system in campus has however only one pyrometer; therefore, it collects angle in horizontal direction.

Pyrheliometer is designed to measure direct solar radiation which results from radiance flux. Radiance flux enters the instrument and is directed to thermopile which converts heat to into electrical signal. That electrical signal is converted via a formula in order to obtain $^{W}/_{m^2}$. In order to obtain beam solar radiation a pyrheliometer was set up on Solys 2 sun tracker. CHP 1 was preferred for high gain and sensitivity, and easily installed on sun tracker.

2.2. Solar Photovoltaic System

2.2.1. Solar Irradiation Data Acquisition and Handling

The circuit based PV model requires inputs of the hourly solar resources and ambient temperatures. For METU NCC, the hourly solar resource model is based on actual solar resource measurements, which have been measured at METU NCC for more than a

year. The solar resource data at METU NCC is being archived with respect to the standard time at the location. The solar resource model for the complete year was thus obtained as the measured data at the campus. The data is taken from the period of June 2013 and May 2014. The solar resource data, average irradiation, is being gathered for every 10 minutes in the campus. To convert it into hourly data, the data was first averaged over an hour and the process was repeated for the entire year. There was an unexpected error during October 2013, some parts of April 2014 and May 2014.

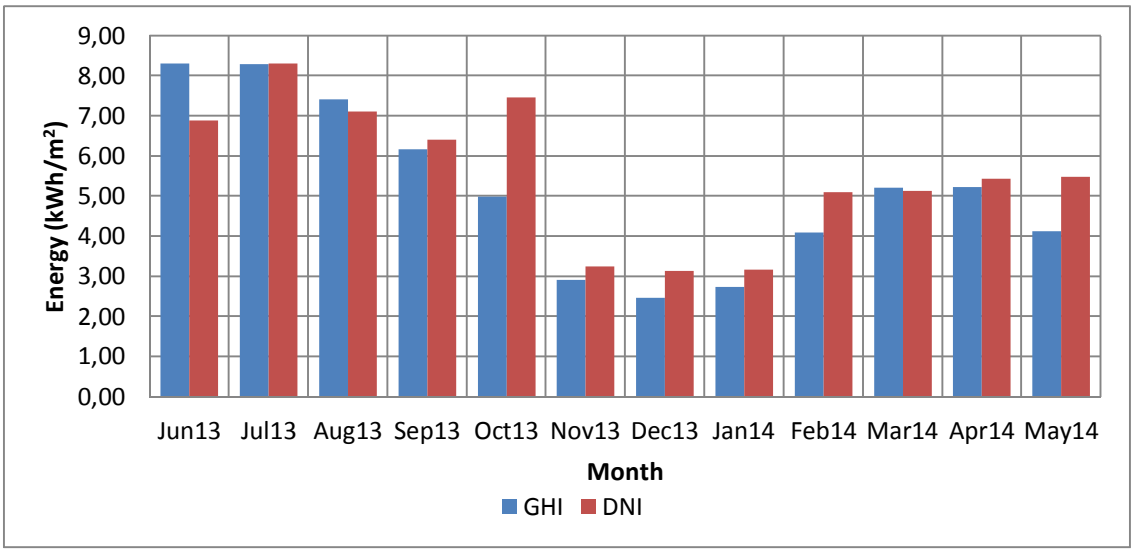

Figure 2: Monthly average global horizontal and direct normal solar irradiation

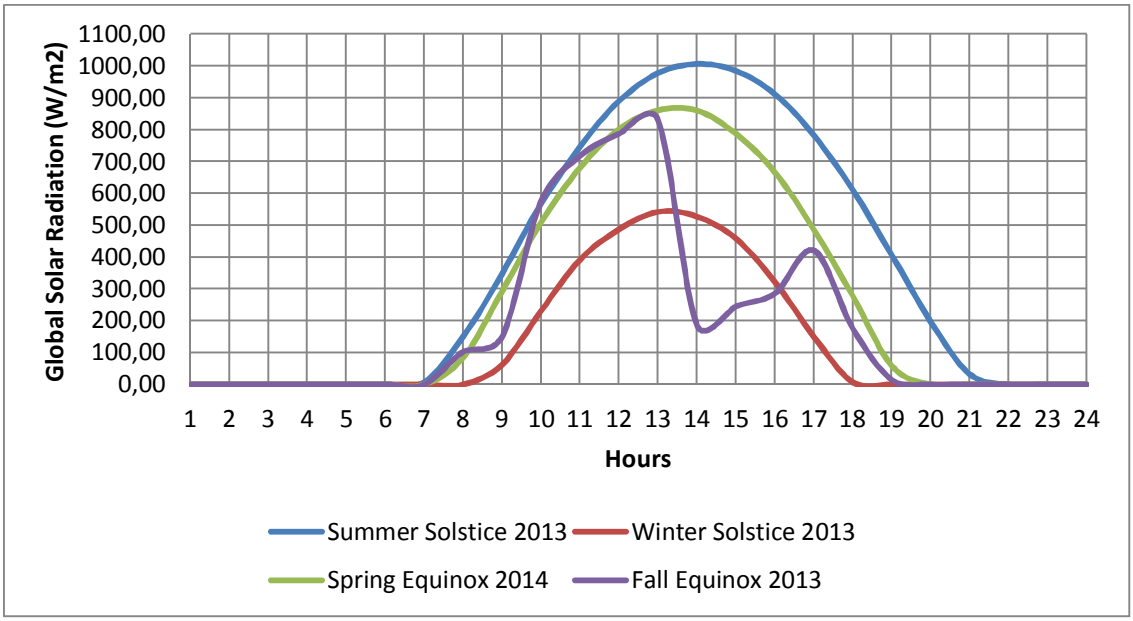

Figure 3: Hourly average of global solar radiation for summer solstice, winter solstice, and spring and fall equinox.

In spite of the fact that both types of solar radiation were high in summer months, it was low in winter months. It is because the day-time in the summer months are more than it is in the winter months.

In Figure 3, average hourly global solar radiation for summer solstice, winter solstice, spring equinox and fall equinox were presented. The day-time increases from winter solstice to summer solstice and vice versa. Area underneath the curve reveals the average daily global solar radiation. The data are recorded all times as daylight savings time (13:00 daylight savings, time is 12:00 standard time). For fall equinox, there was an event, which caused the global solar radiation to be partially reduced to 200 W/m^2. This occurred around 14:00 according to the data taken from 13:10-14:00 for daylight saving time; 12:10-13:00 standard time. Such behavior is expected at times of partly cloudy events.

2.2.2. Reliability of Measured Solar Irradiation Data and Uncertainties in the Dataset

While observing the measured solar resource data of METU NCC, it was observed that the data had some outliers and points that did not look correct. In this part, the reliability of measured data and uncertainties are pointed and discussed.

First of all, the clock on the data acquisition system was wrong during the entire measurement. There is almost one hour difference between the standard time with respect to different time zone. In consequence, the data recorded at all times was considered as the daylight savings time. Second, incident global solar radiation (I) received by a surface is a combination of direct beam radiation (I_b), sky radiation – diffuse radiation – (I_d). The following equation can be used to calculate incident global solar radiation [**32**]:

$$I = I_b \cos\theta_Z + I_d + I_{reflected} \quad (1)$$

where θ is the incidence angle of the sun's rays to the surface and $I_{reflected}$ is neglected. The incidence angle is a function of the sun's position in the sky and the orientation of the surface; while, zenith angle (θ_Z) is the angle between the vertical and the line to the sun, that is, the angle of incidence of beam radiation on a horizontal surface [**32**].

According to the above measuring system described, the problem was occurred depending on the incident angle in summer months (June, July and August). Global horizontal radiation is higher than beam normal radiation from the beginning of the day till 17:00. After that time DNI is higher than GHI till the sunset. One possible reason for this problem is the incident angle is small enough to minimize the value of DNI. To express the definition mathematically: If "cos θ" = "small" (e.g., < 0.5 radian), $I_{b,n} > I$ the problem occurs [**33**]. That explains average global horizontal and beam normal solar radiations are almost the same.

According to the results of this analysis, 380 data points are problematic, namely, they are out of the range. Specifically, the range is determined by the pyrometer and pyrheliometer specification, which is taken as 20 W/m$^{2.}$ Considering that 380 data is about 4.34% of total data gathered from one year, an overall rate of such value is considered acceptable. Moreover, the errors occurred for in the morning times of the months: June 2013, July 2013, April 2014, and May 2014. These data is not accurate due to the fact that multiplication of beam solar radiation with zenith angle is higher than the global solar radiation. There was a measurement error which was defined as 20 W/m^2 and the difference between the global data and beam data is more than 20 W/m^2. Another error occurred in October 2013 such that beam solar radiation was higher than global solar radiation. This can happen on clear days and when the sun is low in the sky. This is significant due to the rapid change in declination.

Another control check was done to figure out the relationship between global and beam solar radiation. Equation (2) indicates another check system for solar noon, which the incidence angle is close to zero (not in the winter, in winter the incidence angle is around 40^0). At solar noon, the global normal solar radiation and beam solar radiation is almost the same, or global normal radiation is higher. If the angle of incidence is zero and neglecting reflected radiation, the control equation is illustrated as:

$$\begin{gathered} if\ \theta_z = 0 \quad then \quad I = I_b + I_d\ ,\ I > I_b \\ if\ \theta_z = Large \quad then \quad I = I_{b,n} \cos\theta_z + I_d \quad , I_{b,n} > I \end{gathered} \tag{2}$$

The results indicate that some of the days, beam solar radiation is higher than the global solar radiation. To manipulate the data, diffuse radiation measurement test was conducted manually. The experiment was conducted for half of an hour of shading global solar radiation so that the beam solar radiation was separated. Measurement of diffuse solar

radiation and beam solar radiation supported average hourly global solar irradiation using the Equation (2).

The second test was done to check global solar radiation and the result indicated of the clearness index. A model, which used incidence angle and extraterrestrial solar radiation, was developed to obtain maximum global horizontal solar radiation on a surface. The equation is expressed as:

$$I_g = I_{g,on}\, x\, cos\, \theta_z \tag{3}$$

Where I_g is the global horizontal solar radiation and $I_{g,on}$ is extraterrestrial solar radiation, which is equal to 1367 W/m^2. This varies with the time of a year by $\pm$ 3.5%. In the model the variation is neglected. Incidence angle was calculated for each hour of a year. To check to data, the condition is written as:

$$\begin{Bmatrix} if\ I_g > I_{g,measured} & TRUE \\ Else & FALSE \end{Bmatrix} \tag{4}$$

The test result indicates measured global horizontal solar radiation is correct. The equation is illustrated in (5) [**34**] & [**35**], and clearness index is found from the analysis as 0.779.

$$K_T = \frac{I_{g,measured}}{I_{g,on}} \tag{5}$$

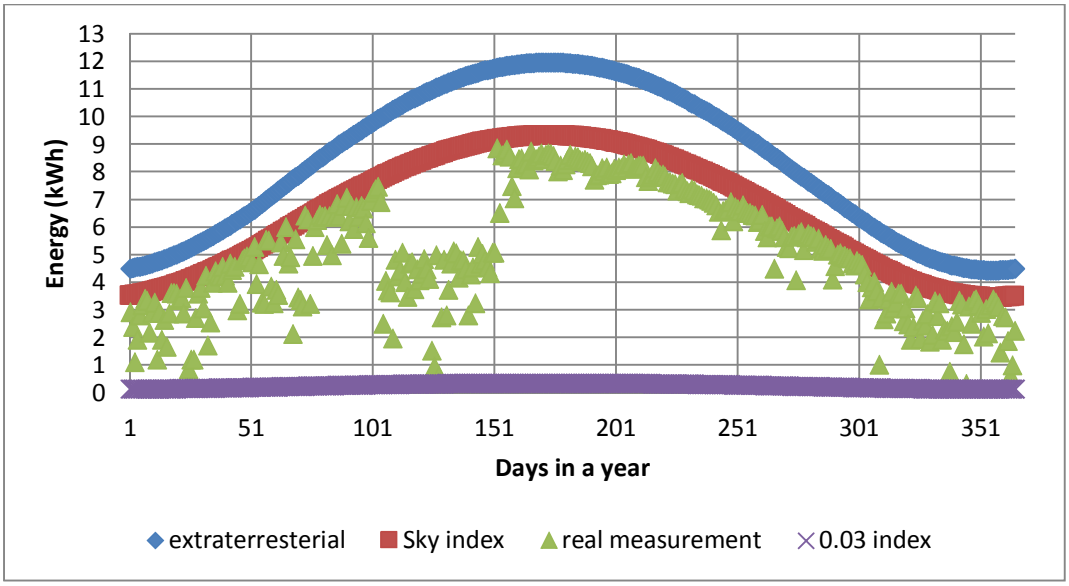

Figure 4: Extraterrestrial solar radiation, clear sky indexed solar radiation, real measurement in METU NCC solar measurement system and 0.03 indexed solar irradiation

In Figure 4, clear sky index result indicates that there is a problem started from the end days of April 2014 and is continuous till May 2014. It is obvious that the results were almost half of the other months. The some parts of April and complete May 2014 data was excluded from the one year data collection due to the corrupted data that is mentioned earlier. Nevertheless, they were included for this study in order to obtain a complete year's data.

One of the recent comprehensive research [**29**], which named methodology to size large scale solar PV installation for institutions with unidirectional metering, has been carried out to find the optimum size of the PV with respect to demand data for the large scale installations. METU NCC solar measurement station data is compared with the data of Serhatköy PV farm solar irradiation measurements. The details of the measurement comparisons of Serhatköy and METU NCC solar data are detailed in Appendix A. It is found from the analysis that the Serhatköy data has one hour lag from METU NCC for summer months. The reason to that is probably the time is not set to daylight saving time for Serhatköy. The author also mentioned that other than the inconsistencies, the data seems to match fairly for presented two locations in Northwestern Cyprus. In METU NCC data on 26th, 27th, 28th and 29th September 2013, there are some inconsistencies in the data range. To note some of the significant aspect of the analysis, the solar resources measured at METU NCC have a good agreement with the solar irradiation measured on Serhatköy, on the cloud-free days. Nevertheless, on cloudy days, measurements do not fit well. Moreover, the author claims that there is no time difference between the two data due to the fact that the daylight savings time ends on 26th October 2013.

2.2.3. Photovoltaic System Overview

The word photovoltaic originated of the two words, photo and Volta. Photo stands for light (Greek phõs, photós: light) and Volta (Count Volta, 1745–1827, Italian physicist) is the unit of the electrical voltage [**36**].

2.2.3.1. Solar Photovoltaic Cell

PV cell have been manufactured with silicon, gallium-arsenide, copper indium and a few other materials [**1**] [**2**] [**36**]. Namely, understanding the p-n junction is necessary to understand how a PV cell converts sunlight into electricity. The light photons with energy higher than the band-gap energy produces electrons in the material described in Figure 5. If the closest electric field is activated, the electrons in the conduction band can continuously move to a metallic contact [**1**]. The electric field created by the different regions in the semiconductor described as p-n junction [**36**]. In Figure 5, PV cell has an electric contact on its top and bottom in order to capture the electrons. Electrons go out of the n-side to the load within the wire, when PV cell delivers power, and then come back to the p-side. In order to note a significant point, current flow is opposite to the directions of electron flow.

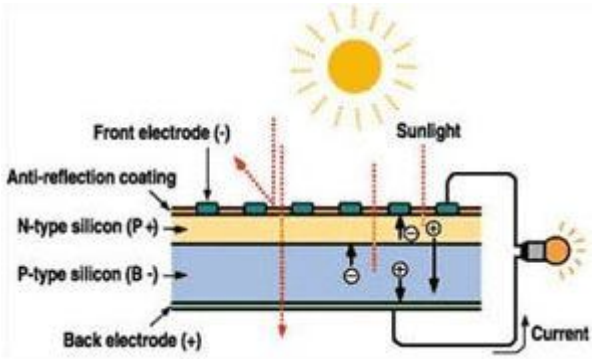

Figure 5: P-N junction illustration of Photovoltaic Cell [**37**]

2.2.3.2. Solar Photovoltaic Module/Array

A PV array is made with series and parallel connections of multiple cells/modules. Namely, it is an interconnection of cells/modules. The power delivered from the single cell is insufficient to match the demand. The connection of the cells and modules in a matrix increases the output power delivered to the system. The combination diagram can be illustrated in Figure 6. Mathematical details are explained in Section 2.2.4.

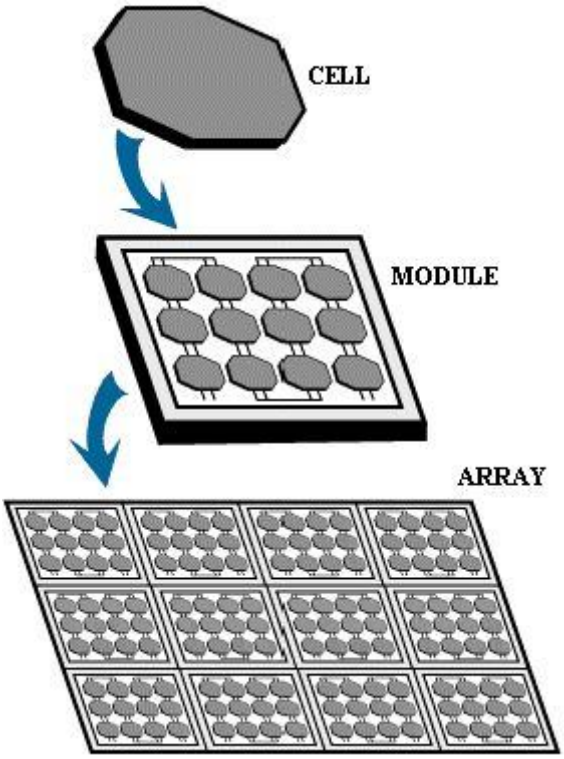

*Figure 6: Photovoltaic Hierarchy: Cell, Module and Array [**38**]*

2.2.4. Circuit Based Mathematical Modeling of Photovoltaic System

A solar module is series and parallel combinations of a multiple solar cell. Solar cell or module can be considered by utilizing a current source, a diode, a series resistor and a parallel resistor [**39**] [**40**] [**41**] [**42**] [**43**] [**44**] [**45**] [**46**] [**36**] [**47**] [**48**]. This model is known as a single diode solar cell or module model. Two diode models are also available but only single diode model is considered in the scope of this research [**49**]. Because, single-diode model has more straightforward mathematical description of a solar cell. Model involves a photocurrent, two diodes, a series resistance and a shunt resistance. The I-V characteristics curve is difficult to find out due to the non-linear characteristic of the equation. In other words, there are limitations of using two diode solar cell models; therefore, this model is rarely used in the literature [**49**]. Another comprehensive research has been done to carry out the accuracy of both single diode and two diode circuit models. The comparison indicated that both mathematical models have the almost same accuracy in the measurement range of environmental conditions [**49**]. Hence, for simplicity purposes, and as 2-diode

model does not provide significant contribution to the goal of this research, two diode model is not used. Single diode model is employed instead within the scope of this study.

The equivalent circuit diagram is illustrated in Figure 7. It consists of a photo current source, a diode, a resistor (R_{SH}) shunt connected to the diode expressing the leakage current and a series resistor (R_S) at the end of the system describing an internal resistance to the current flow.

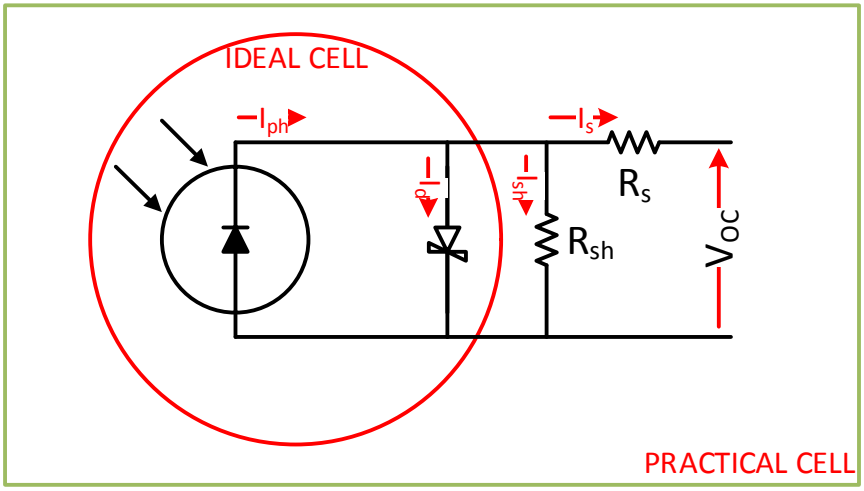

Figure 7: General model of a PV cell/module in a single diode model

Electrical characteristic of a PV module/cell illustrated as PV cell output current (I) and output voltage (V). The output current depends on mostly the solar irradiance (S), temperature (T_{CELL}) of the cell and material characteristic [**1**]. Based on the model described in Figure 7, the ideal cell model is described first in order to explain the fundamental behavior of the PV module. The practical model is explained next as it provides more idealistic behavior.

2.2.4.1. Ideal Cell Model

Referring to the Figure 7, ideal cell model can be represented by a photo current source connected in shunt with a rectifying diode (Shockley diode). In other words, the series and shunt resistances determined as Rs is very small (Rs = 0) and Rsh is very large (Rsh = ∞). The corresponding I-V characteristics of ideal cell based on the Kirchhoff's first law can be expressed as:

$$I = I_{ph} - I_d \tag{6}$$

where:

$$I_{ph} = \left(I_{scr} + k_i(T - T_r)\right)\left(\frac{S}{S_r}\right) \tag{7}$$

$$I_d = I_o\left(e^{\frac{qV}{kT}} - 1\right) \tag{8}$$

where I_{ph} is a light-generated current, i.e. photo-current, q is an electron charge, k is the Boltzmann's constant, T is the cell's working temperature and S is the irradiance. I_{ph} is the photo-current resource depends mostly on cell working temperature and solar irradiance [**1**]. Considering the Equation (7), solar irradiation is the main factor on Iph. Nevertheless, increasing temperature goes up the photo current if there is sufficient solar irradiation. On the other hand, I_d is the diode current and temperature has an exponential factor it. The solar irradiance and temperature effects are considered within the scope of this study.

2.2.4.2. Practical Cell Model

In practice, due to leakage factors, power efficiency is degraded, and due to introduced leakage factors, relevant mathematical expressions becomes more complicated. Again referring to the Figure 7, practical solar cell model can extract more realistic results due to the effect of leakage current analysis expression. In other words, the I-V characteristic of a solar cell in practice differs from ideal characteristics, and the circuit may also include series resistance (R_S) and shunt resistance (R_{SH}). Based on Kirchhoff's current law and considering the extensive researches [**1**] [**45**] [**36**] [**40**] [**43**], I-V characteristic of a cell/module can be indicated in following set of equations:

$$I = I_{ph} - I_d - I_{sh} \tag{9}$$

where:

(10)

$$I_{ph} = \left(I_{scr} + k_i(T - T_r)\right)\left(\frac{S}{S_r}\right) \tag{11}$$

$$I_d = I_o\left(e^{\frac{qV}{kT}} - 1\right) \tag{12}$$

$$I_0 = I_{0,r}\left(\frac{T}{T_r}\right)^3 \exp\left[\frac{qE_g}{nk}\left(\frac{1}{T_r} - \frac{1}{T}\right)\right] \tag{13}$$

$$E_g = E_{g0} - \frac{\alpha T^2}{T+\beta} \quad (14)$$

$$V_t = \frac{nkT}{q} \quad (15)$$

$$T_r = (T_{r1} - 32) + 273 \quad (16)$$

$$V_{sh} = V_d \quad (17)$$

$$V_d = V + IR_s \quad (18)$$

$$I_{sh} = \frac{V_{sh}}{R_{sh}} = \frac{V_d}{R_{sh}} = \frac{V + IR_s}{R_{sh}} \quad (19)$$

thus;

$$I = I_{ph} - I_d - I_{sh} \quad (20)$$

$$I = \left(I_{scr} + k_i(T - T_r)\right)\left(\frac{S}{S_r}\right) - I_o\left[\exp\left(\frac{V+IR_s}{nkT/q}\right) - 1\right] - \frac{V+IR_s}{R_{sh}} \quad (21)$$

Equation (21) is done with 5 nodes. In fact, a comprehensive work [**49**] compared 5-node and 7-node solving. Moreover, another extensive study [**45**] investigated four and five parameter models. The results indicated that it improved the accuracy of the curve by 1% only, while making the calculation time extremely long. The model parameters can be determined by the PV technology. The ideality factor (n) depends on the PV technology, listed in Table 4. Also, E_{g0}, α and β are the parameters differs from utility type of technology and are listed in Table 5. E_g is the band gap energy of the semiconductor.

*Table 4: Factor (n) dependence on PV technology [**40**]& [**50**]*

Technology	n
Si-mono	1.2
Si-poly	1.3
a-Si:H	1.8
a-Si:H tandem	3.3
a-Si:H triple	5
CdTe	1.5
CIS	1.5
AsGa	1.3

*Table 5: The parametersE_{g0}, α and β in Equation (14) [**39**]*

	$E_g(T=0K),eV$	$\alpha\ x\ 10^{-4}, {}^{eV}/_{K^2}$	β, K
Si	1.17	4.730	636
AsGa	1.52	5.405	204
InP	1.42	4.906	327

The shunt resistance R_{sh} is inversely proportional to shunt leakage current to the ground; therefore, the shunt-leakage resistance can be assumed as infinitely large. However, the variation in the series resistance affects the PV output power significantly.

The other point is that the single solar cell is not strong enough to generate the entire capacity of the system. In many models that are present in the literature, the series and parallel combination of the cells/modules are attached between each other, the combination is illustrated in Figure 8.

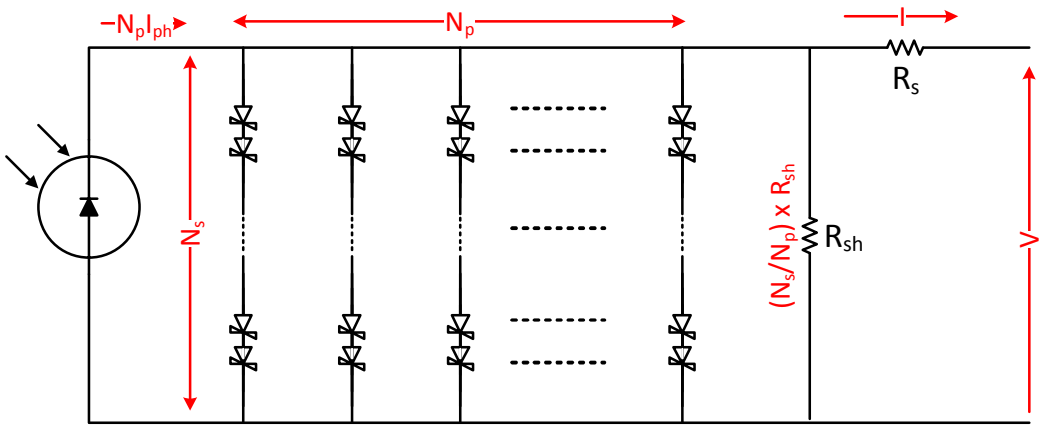

Figure 8: General model of an equivalent PV array

This model describes the electrical behavior and determines the relationship between the output voltage and current. Series combination increases the module voltage; on the other hand, the parallel one increases the current. In this combination model, the set of equation of a single diode model can be summarized in the following equation:

$$I = Np\left\{\left(I_{scr} + k_i(T - T_r)\right)\left(\frac{S}{S_r}\right)\right\} - Np\, I_o\left\{\left[\exp\left(\frac{\frac{V}{N_s} + \frac{IR_s}{N_p}}{nkT/q}\right) - 1\right]\right\} - \left\{\frac{\frac{N_p}{N_s}V + IR_s}{R_{sh}}\right\} \quad (22)$$

The behavior of the proposed PV model and its I-V and P-V characteristics are applied to the MATLAB based on the set of equations described. Classical parameters are described, i.e. short circuit current, open circuit voltage and maximum power. The reference solar PV module was selected from Serhatköy PV farm Module, which is ANEL 205 NEC, and the module characteristics are presented in Table 6. Serhatköy PV farm data was used in the scope of the thesis to evaluate the accuracy of the model.

Table 6: Reference PV module Characteristics (e.g. Serhatköy Power Plant Modules

Maximum Power	205	Wp
Voltage at Max Power	26.39	V
Current at Max Power	7.8	A
Open Circuit Voltage	33.08	V
Short Circuit Current	8.33	A
Panel Efficiency	13.7	%
Power Tolerance	3	%
Operating Temperature	-40~85	C
Temperature coefficient of Pmax	-0.39	%/C
Temperature coefficient of Voc	-0.3	%/C
Temperature coefficient of Isc	0.047	%/C
Maximum system Voltage	1000	V
Cell Type	polycrystalline Silicon	

Referring to the Table 4, system is polycrystalline silicon; therefore, the ideality factor (n) is chosen as 1.3, which is described in Table 4. Maximum voltage, current and power at standard test conditions (STC, AM = 1.5; T = 25 C; S = 1000 W/m^2) is 26.39 V, 7.80 A and 205 W_p respectively. Temperature coefficient of short circuit current is another significant parameter of description and it is 0.047 %/℃. Lastly, the maximum system voltage, which is the parameter used for the series connection of the PV modules in utility, is 1000V. Namely, maximum system voltage divided by open circuit voltage gives the

maximum series connection number and it is found as 30. In addition, bandgap energy of silicon material referring to the Table 5 is 1.17 eV; α and β characteristics are $4.730x10^{-4}eV/K^2$ and 606 K respectively. I-V and P-V characteristic diagram of ANEL 205 NEC solar module using proposed mathematical model are shown in Figure 9 and Figure 10.

There is a logarithmic relationship between voltage and current; the diagram is inversely equal to the diode I-V characteristic. Referring to the Figure 9, short circuit current is 8.5 A and open circuit voltage is 35 V. Power is equal to the multiplication of voltage and current. Considering the results, the maximum power is calculated as 297.5 W; nevertheless, the maximum power is not equal to the open circuit voltage (V_{oc}) and short circuit current (I_{sc}) . Connecting a load to the system changes the output characteristic. In addition, logarithmic relationship of the I-V characteristic indicates where the maximum power is close to V_{OC} and I_{SC}. Referring to the Figure 10, the maximum power is the pick point of the curve shape, which is equal to 205 W_p. For maximum power, the characteristic voltage is 26.5 V and current is 7.73 A.

R_S and R_{SH} are calculated iteratively. The goal is to find the values of R_S and R_{SH} which makes the mathematical P-V curve peak at the (V_{mp}, I_{mp}) point by iteratively increasing the value of R_S while simultaneously calculating the value of R_{SH} with Equation (23). The initial conditions for R_S and R_{SH} are shown in Equation (24). The iterative method gives the solution R_S = 0.389 Ω and R_{SH} = 182.321Ω.

$$R_{SH} = \frac{V_{MP}(V_{MP} + I_{MP} R_S)}{V_{MP} I_{MP} - V_{MP} I_0 \left[\frac{(V_{MP} + I_{MP} R_S)q}{N_S \, x \, \alpha \, x \, k \, x \, T}\right] + V_{MP} \, x \, I_0 - P_{MP}} \tag{23}$$

$$R_S = 0;\ R_{SH,min} = \frac{V_{MP}}{I_{SC} - I_{MP}} - \frac{V_{OC} - V_{MP}}{I_{MP}} \tag{24}$$

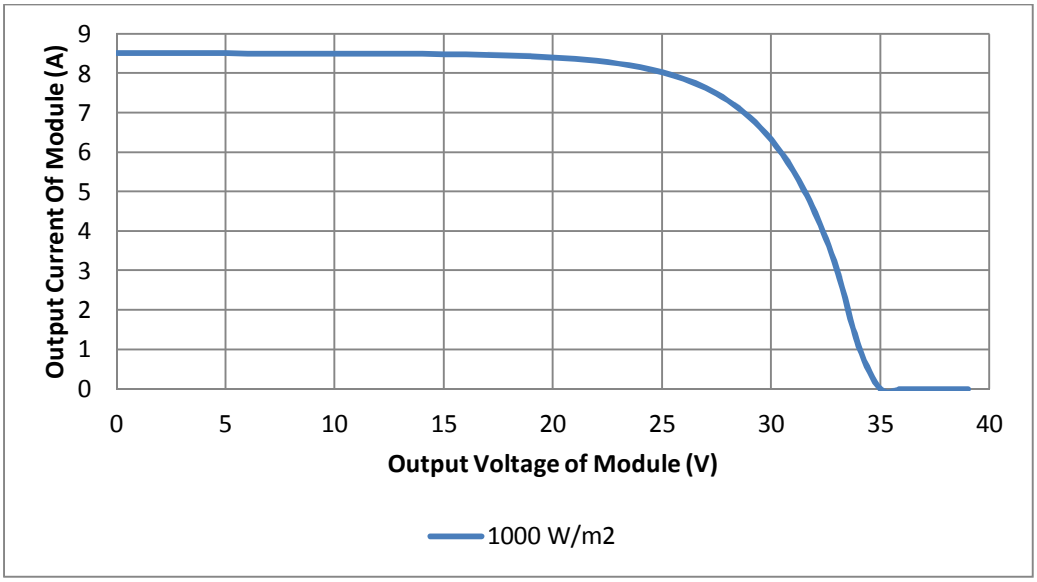

Figure 9: I-V curve of the proposed PV model under standard test conditions

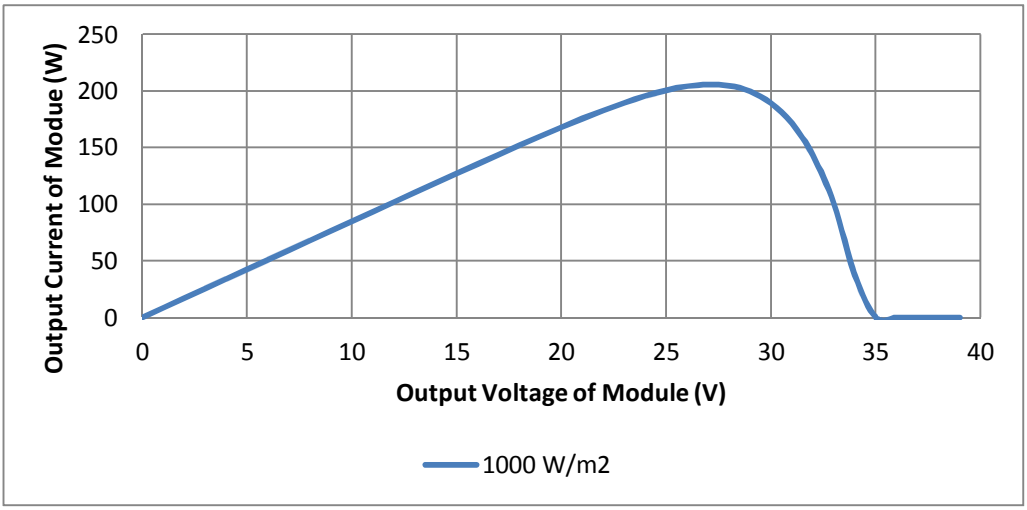

Figure 10: P-V curve of the proposed PV model under standard test conditions

In this model, effects of variation of solar irradiance are considered at constant temperature. The temperature is chosen as the standard test condition temperature, which is 25 C. The I-V and P-V characteristic diagram for each solar irradiance value in the same graph as indicated in Figure 11 and Figure 12, respectively. In order for each solar irradiation, the rate of change in voltage is really low in comparison with the current. When the irradiance, for instance, is 500 W/m^2, the open circuit voltage is 33 V yet the current is

4.25 A. Rate of change in the voltage and current also decreases the output power. Referring to the Figure 12, the power is half when the irradiation is 500 W/m^2.

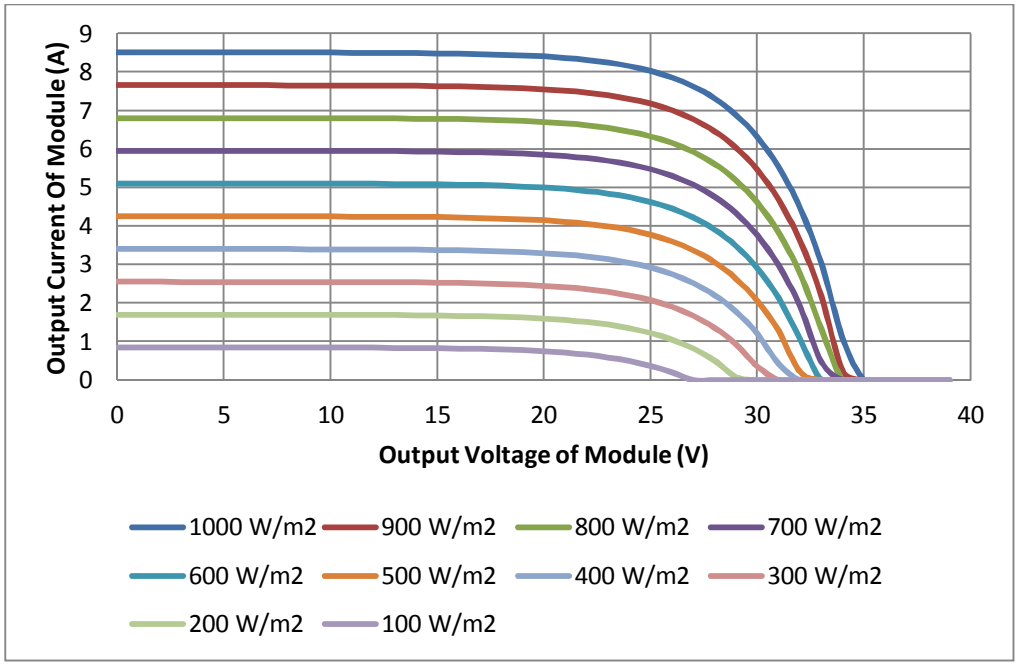

Figure 11: I-V curve of the proposed PV model under different solar irradiation condition

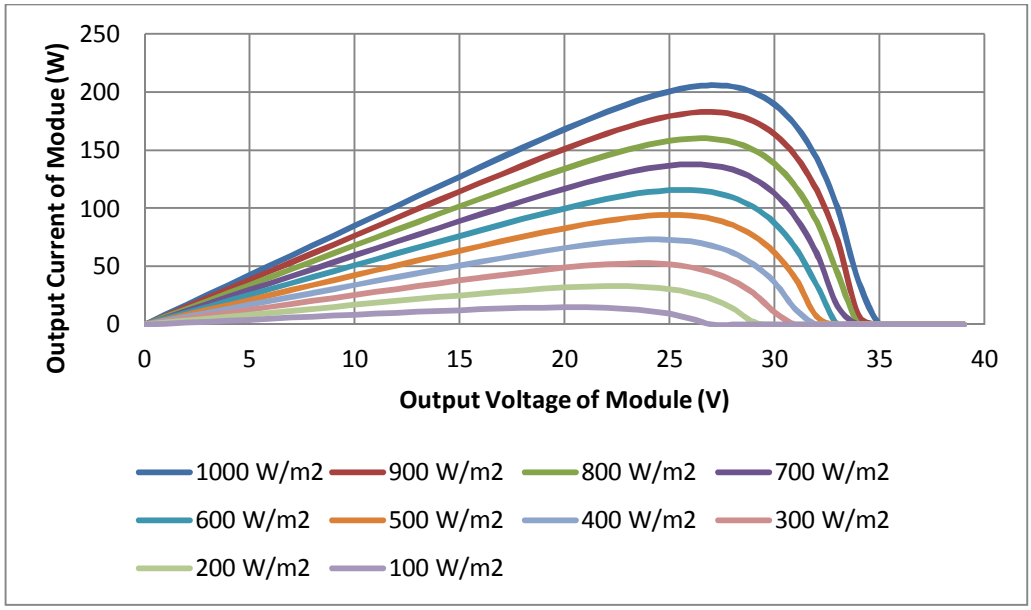

Figure 12: P-V curve of the proposed PV model under different solar irradiation condition

2.2.5. Global Tilted Irradiation (GTI) Calculation Using GHI and DNI

This part of the analysis is inspired from [**32**] & [**33**]. Day number is a number that converts a month-day to a day of a year (i.e. n = 1 for January 1, n = 32 for February 1, etc.). In other words as it is known, a year has 365 days except leap year so this model calculates a day in a month to convert which day it will presents in a year.

Earth is closer to sun in northern hemisphere in winter which causes variations and shows the elliptical orbit of the earth.

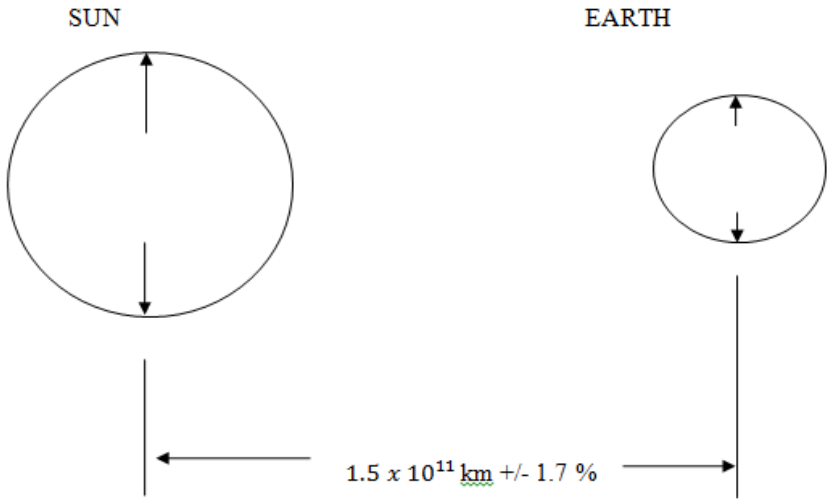

Figure 13: Distance between the Sun and Earth

$$G_{ON} = G_{SC}\,[1 + 0.033\cos(\frac{360n}{365})] \tag{25}$$

where $1 \leq n \leq 365$.

Thus, G_{SC} = 1367 $\frac{W}{m^2}$ (This varies about +/- 3,3 over the year, but although it is important to integrate this to the simulations, it will not be able to be done).

Another important factor is hour ending represents mean values of the given period (i.e. hour = 1 and hour = 2; hour ending = 1.5). However, the data, which was collected, is a ten-minute period so it was assumed that each ten-minute represents its mean values. This is indicated by the following equation:

$$t_{\text{hour ending}} = t_{\text{hour}} + \frac{t_{\text{minutes}}}{60} \tag{26}$$

Example: Hour = 3 and Minutes = 20: Hour Ending = $3 + \frac{20}{60} = 3.333$

There is two important value which are named as B value and E value. B value is an angular representation of a year which is used instead of a day representation to show the Earth's place through the Sun. It can be expressed as:

$$\text{B value} = (n-1)\,x\,\frac{360}{365} \tag{27}$$

Where n is day number of a year. In addition to B value, E value is specific value and it can be easily calculated by B value. It is given by the following equation:

$$\begin{aligned}\text{E values} = {} & 229.2\,x\,(7.5x10^{-5}) + 0.001868\,x\cos(\text{B values}) \\ & - 0.032077\,x\sin(\text{B values}) \\ & - (0.014615\,x\cos(2\,x\,\text{B values}) \\ & - 0.04089\,x\sin(2x\,\text{B values})\end{aligned} \tag{28}$$

Solar time is a reckoning of the passage of time based on the Sun's position in the sky. The fundamental unit of solar time is the day. Two types of solar time exist, apparent solar time (sundial time) and mean solar time (clock time). Apparent solar time or true solar time is based on the visual motion of the actual Sun. It is based on the apparent solar day, the interval between the two successive returns of the Sun to the local meridian. Solar time can be crudely measured by a sundial. Mean solar time is the hour angle of the mean Sun plus 12 hours. The duration of daylight varies during the year but the length of a mean solar day is nearly constant, unlike that of an apparent solar day. To calculate solar time we need to find the "lst" and "lloc" values of the given location. The exact presentation of given location is required. These values are specified according to the location. The formulation can be demonstrated by:

$$\text{lst} = \begin{cases} 360 - (\text{TZx15}) & \text{if TZ} > 0 \\ -\text{TZ} & \text{if TZ} < 0 \end{cases} \tag{29}$$

$$\text{lloc} = \begin{cases} 360 - \text{longitude} & \text{if Lew} = 'E' \\ \text{longitude} & \text{if Lew} = 'W' \end{cases} \quad (30)$$

TZ is "Time Zone" and Lew is "Longitude East West". Considering Equation (29) and (30) solar time can be easily extracted and can be illustrated as:

$$\text{ST} = \text{Hour Ending} + \frac{1}{60}(4\text{x}(\text{lst} - \text{lloc}) + \text{E value}) \quad (31)$$

ST presents "Solar Time" in above equation. Furthermore, the solar hour angle is the angular displacement of the sun in the east which is negative in the morning or in the west, which is positive in the afternoon, of the local meridian. The solar hour angle is equal to zero at solar noon and varies by 15 degrees per hour from solar noon. For example, at 7 a.m. (solar time) the hour angle is equal to –75° (7 a.m. is five hours from noon; five times 15 is equal to 75, with a negative sign because it is morning). The sunset hour angle ω_s is the solar hour angle corresponding to the time when the sun sets. It is given by the following equation:

$$\cos\omega_s = -\tan\varphi \tan\delta \quad (32)$$

Where δ is the declination, calculated through equation (46), and φ is the latitude of the site, specified by the user. The declination is the angular position of the sun at solar noon, with respect to the plane of the equator. Its value in degrees is given by Cooper's equation:

$$\delta = 23.45 \sin\left(2\pi\frac{284+n}{365}\right) \quad (33)$$

Declination varies between -23.45° on December 21st and +23.45° on June 21st.

where

$-23.45° < \delta < 23.45°$

$\delta = 23.45°$ (Summer Solstice – June 21st)

$\delta = 0°$ (spring/fall equinox – March 20th/Sept 23rd)

$\delta = -23.45°$ (Winter Solstice – Dec 21st)

To sum up all calculation, there are two important angles: zenith angle and azimuth angle. These analysis converge to these two angular representations. These representations refer to the spherical coordinate system. The zenith is an imaginary point directly "above" a particular location, on the imaginary celestial sphere. "Above" means in the vertical direction opposite to the apparent gravitational force at that location. The solar zenith angle is the angle measured directly from overhead to the geometric center of the sun's disc, as described using a horizontal coordinate system.

$$\cos\theta_z = \cos\varphi\ \cos\delta\ \cos h + \sin\varphi \sin\delta \tag{34}$$

On the other hand, solar Azimuth angle defines in which direction the Sun is, whereas the solar zenith angle defines how high the Sun is, namely, elevation is the complement of the zenith angle. It is defined as:

$\gamma<0$ in the morning

$\gamma>0$ in afternoon

$\gamma=0$ at solar noon

$$\gamma_s = \text{sign}\,(\omega)\left|\cos^{-1}\left(\frac{\cos\theta_z \sin\emptyset - \sin\delta)}{\sin\theta_z \cos\emptyset}\right)\right| \tag{35}$$

Where;

$$\text{sign}\,(\omega) = [\ 1 \text{ if } \omega > 0 \text{ and } -1 \text{ if } \omega < 0 \tag{36}$$

At the end on all theoretical background of angular calculation, solar zenith and solar azimuth angle is calculated for each hour of a year. By using these spherical coordinates and most importantly adding the DNI factor to the calculation, GTI of any near location can be estimated and the estimation formula is illustrated as:

$$\cos\theta_\beta = \cos\theta_z \cos\beta + \sin\theta_z \sin\beta \cos\gamma - \gamma_s \tag{37}$$

$$GTI_\beta = \begin{Bmatrix} \text{DNI}\cos\theta_\beta + I_d\left(\frac{1+\cos\beta}{2}\right) & \text{if} \quad \theta_\beta < 90 \\ I_d\left(\frac{1+\cos\beta}{2}\right) & \text{if} \quad \theta_\beta > 90 \end{Bmatrix} \tag{38}$$

3. METHODOLOGY FOR WIND ENERGY

3.2.1. Wind Energy Measurement System

In this part of the thesis, wind data measuring systems that currently used in METU NCC are focused. A sixty-meter wind tower was installed on METU NCC to gather wind data. The tower involves four anemometers, which are used for wind speed measurement, at 30^{th}, 40^{th}, 50^{th} and 60^{th} meters of the tower, two wind vanes, which are used for wind direction measurement, at 48^{th} and 58^{th} meters of the tower, a thermometer, a barometer and humidity. These are the devices to determine basic weather condition of a specific field. Wind Tower devices were demonstrated in Table 7and the schematic view of tower is indicated in Figure 14.

Table 7: Wind Tower Devices

Number	Device
1	Anemometer
2	Wind Vane
3	Shield
	Humidity
	Thermometer
4	Barometer
	Data Logger
	Solar Charge Controller
	Battery
5	GPS-GPRS Antenna
6	Solar Panel
7	Paratoner
8	Warning Lamp

The tower can be investigated in eight different parts of which were located as in Figure 14. The Part 1 involves anemometers at 30^{th}, 40^{th}, 50^{th} and 60^{th} meters of the tower and the Part 2 involves wind wanes used for wind direction at 48^{th} and 58^{th} meters of the tower. Part 3 includes a shield, humidity and thermometer. Barometer, data logger, solar charge controller and battery are placed in the box of Part 4; furthermore, a solar panel is placed in Part 6. Solar charge system is necessary for supplying energy in the remote areas

as the tower is placed approximately 2 kilometer out of campus area. A GPRS system is located in Part 5 to make a connection between the computer and the tower. Lastly it is strictly important to install a paratoner system and warning lamp at the top of the tower to protect it from lightning and to warn flying objects.

Anemometer is a device which was used for measuring wind speed. Wind flowing cause rotation on the axis of a plate, which was connected to a simple motor. The rotation turns the mill of the motor and thus it produces electricity. There is a relationship between the wind speed and amplitude of generated electricity from the motor. Except from the anemometer wind vane determines the direction of wind speed. Since wind is a vector, the velocity of the wind is proportional to both speed and direction. Wind vane is a device which was used for measuring wind direction. Thermometer is a kind of device used for measuring the temperature in the air for a specific field. It is necessary to get information about temperature for weather stations. Barometer specifically used for measuring the air pressure, namely, it is a device for measuring air pressure. The last equipment of the weather station in METU NCC is hygrometer which is used for measuring humidity in the air.

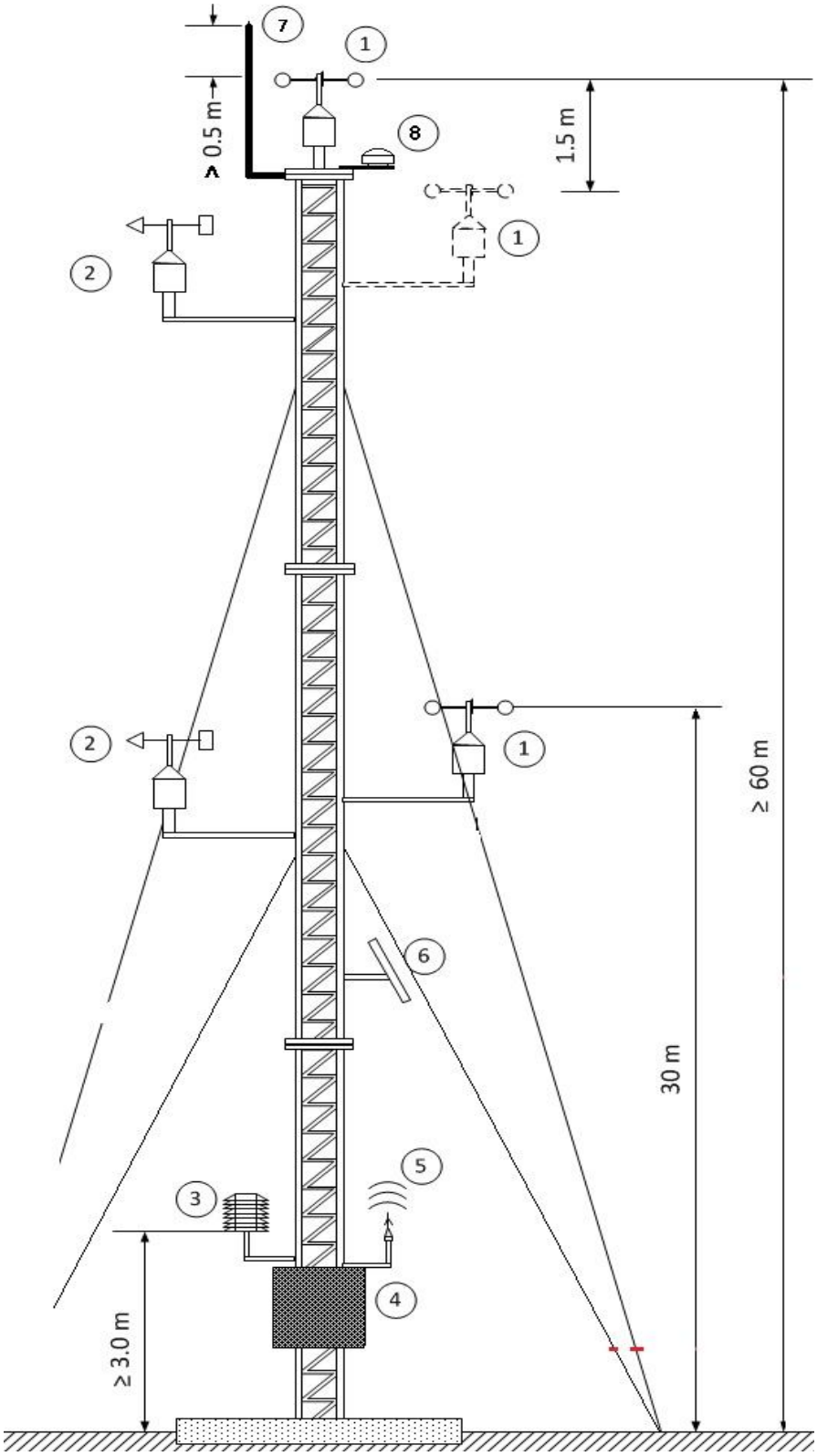

Figure 14: Wind Tower Model

3.2.2. Wind Data Acquisition

Wind is caused by air moving from higher pressure to lower pressure in the atmosphere. The speed of wind is measured by anemometer and it has a relationship with respect to height. METU NCC installed a wind energy program to measure real-time wind speed, wind direction, air pressure, temperature and humidity. Wind speed of 30th, 40th, 50th and 60th meters of wind tower were considered. However, 40th meter anemometer has mechanical problems during a one-year measurement period; hence it is not included in this analysis. The wind data was collected for the period of March 2013 to February 2014. To analyze one-year wind data, a mathematical model from the literature was programmed. Example of the wind speed dataset was indicated in the figures. Monthly average wind speed of 30th, 50th and 60th can be illustrated:

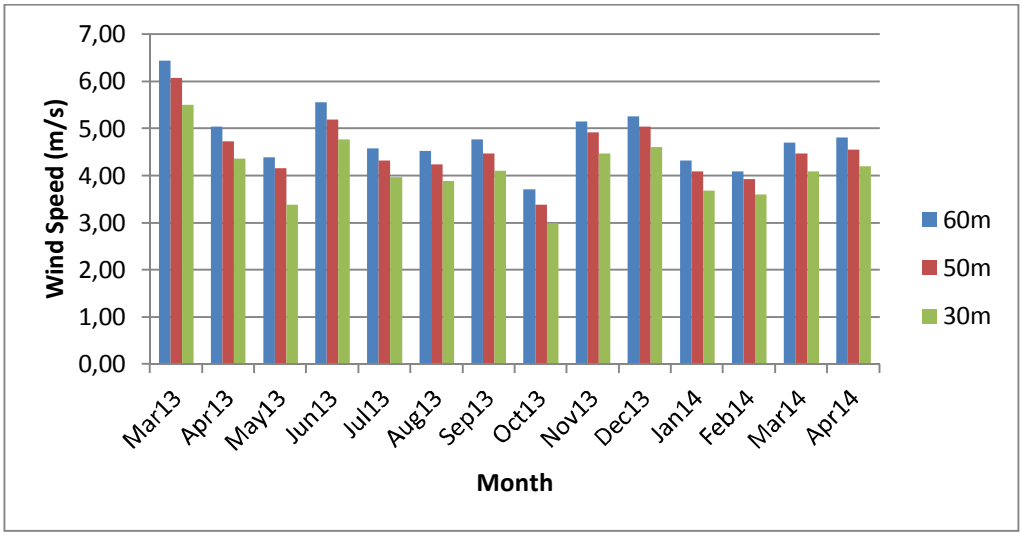

Figure 15: Average monthly wind speed distribution of wind measurement tower at 30th,50th and 60th meters

Figure 15 indicates the monthly average wind speed of METU NCC wind tower. To demonstrate in more detailed information about wind data gathered from METU NCC wind tower, average daily wind speed variation in June 2013 is illustrated in Figure 16 and average hourly wind speed variation on 3rd of June 2013 is illustrated in Figure 17.

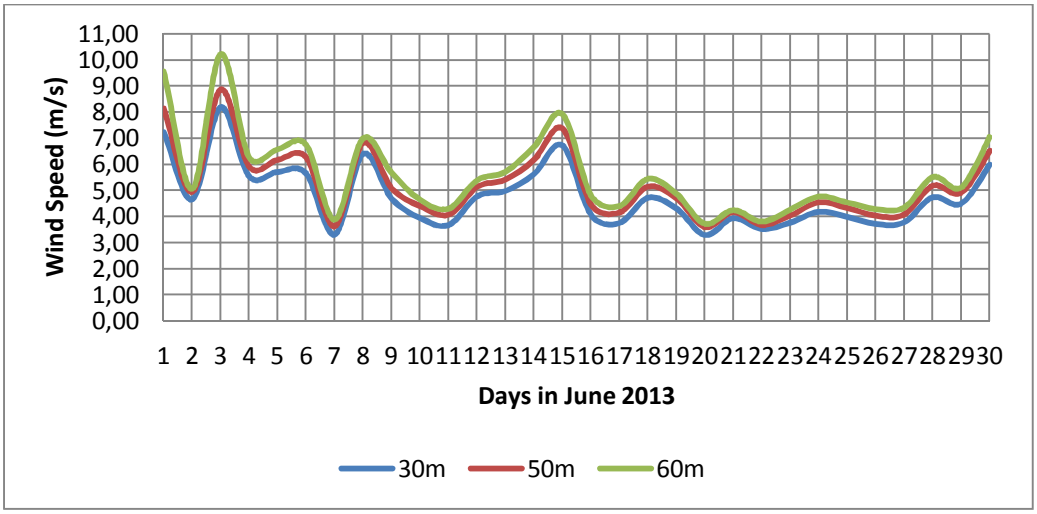

Figure 16: Average daily wind speed distribution in June 2013

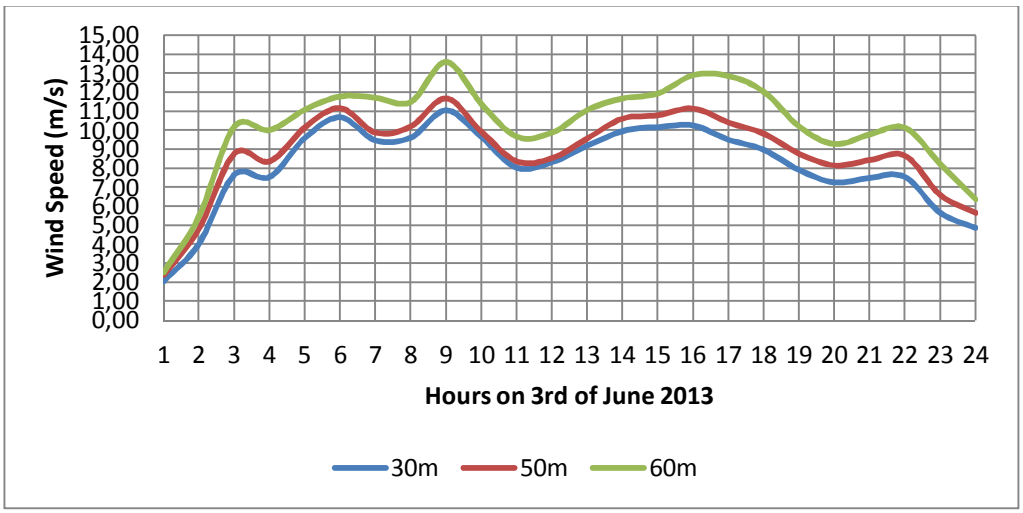

Figure 17: Average hourly wind speed distribution on 3rd of June 2013

At very low wind speeds, there is insufficient torque exerted by the wind on the turbine blades in order to make them rotate. As speed increases; however, wind turbine begins to rotate and generate electricity. The speed at which the turbine first begins to rotate and generate electricity is called cut-in speed and is typically between 3 and 4 meters per second.

As the wind speed increases above cut-in speed, the level of electrical output increases rapidly. After a typical value, generator reaches its limit. It is called rated wind speed of the turbine and typically it is somewhere between 12 and 17 meter per second. At

higher wind speeds, the design of the turbine is arranged to limit the power to this maximum level and there is no further rise in the output power. How this is done varies from design to design but typically with large turbines, it is done by adjusting the blade angles so as to keep the power at a constant level.

The speed increases above the rated output wind speed, the forces on the turbine structure continue to rise and, at some point, there is a risk of damage to the rotor. As a result, a breaking system is employed to bring the rotor to a standstill. This is called the cut-out speed and is usually around 25 meter per second.

3.2.3. Wind Data Correlation

Correlation coefficient is a value which reveals the dependence of one variable on another. In this study, Pearson correlation coefficient was analyzed to test the relationship between wind speeds from one meter to another. It has been categorized into three parts:

Positive correlation is that the other variable has a tendency to increase

Negative correlation is that the other variable has a tendency to decrease

No correlation is that the other variable has a tendency to increase

The well-known dependent analysis between the two stochastic processes is Pearson correlation coefficient. Basically, it is obtained by the covariance of the two stochastic processes over by the multiplication of their standard deviation, mathematically, it can be expressed as:

$$\mathrm{corr}(X, Y) = \frac{\mathrm{cov}(X,Y)}{\sigma_x \sigma_y} \tag{39}$$

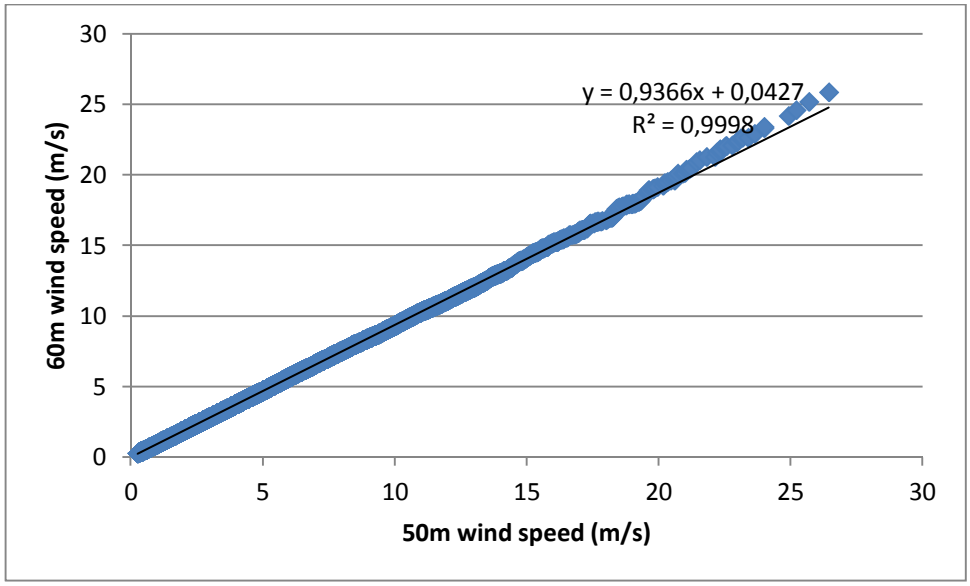

Figure 18: 60 meter and 50 meter wind correlation

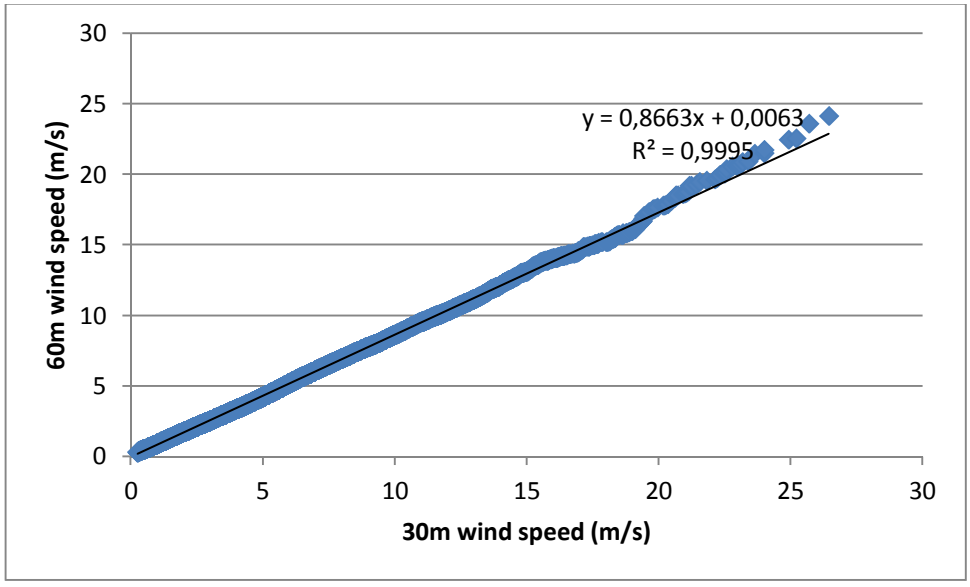

Figure 19: 60 meter and 30 meter wind correlation

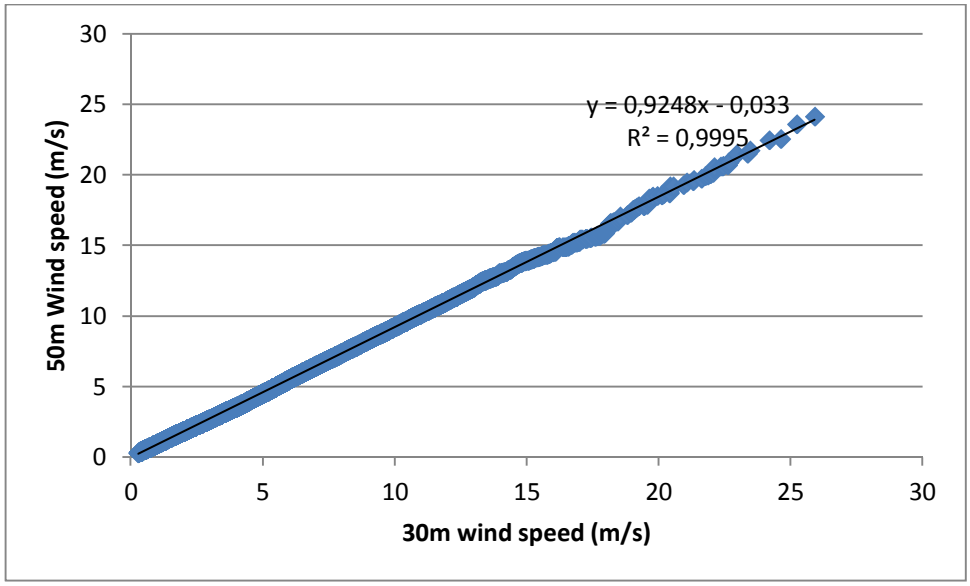

Figure 20: 50 meter and 40 meter wind correlation

Figure 18, Figure 19 and Figure 20 above present the wind data correlation. The results were demonstrated as:

- 60 meter vs 50 meter measurements correlation coefficient is 0.9366 and the R-square value is 0.9998 which are both close to one. Therefore, there is positive correlation.
- 60 meter vs 30 meter measurements correlation coefficient is 0.8663 and the R-square value is 0.9995 which are both close to one. Therefore, there is positive correlation.
- 50 meter vs 30 meter measurements correlation coefficient is 0.9248 and the R-square value is 0.9995 which are both close to one. Therefore, there is positive correlation. All three analyses have the similar results which is significant to show there is positive relationship between the variables of stochastic processes. Hence, these are not independent from each other.

3.2.4. Wind Turbine Electrical Energy Generation, Efficiency and Power Coefficient

There are some fundamental concepts in order to calculate energy extracted from wind. The equation that is used to find the power obtained by a wind turbine is given as [**2**]:

$$P = \tfrac{1}{2} \rho A v^3 C_p \quad (40)$$

ρ = density of the air (kg/m^3)
V= Velocity of the air (m/s)
A= Span Area of the turbine (m^2)
P = Output power (W)
C_p = Power Coefficient

Equation ((40) shows the power obtained from a wind turbine has a cubic relation with wind speed. Therefore, hourly data of wind speed obtained from the measurements can be very useful in order to find the amount of predicted wind energy. If the wind speed is in meters per second, the air density is in kilograms per cubic meter and the rotor swept area is in meter squire, then the available power is in Watts. The efficiency (μ), namely capacity factor of the wind turbine, is simply referred as the actual power, which is delivered from the wind turbine, divided by the available power.

3.2.5. Betz Limit Law on Wind Turbines

Wind machines performance is defined by Betz's theory. Albert Betz was a German physicist who calculated wind turbine power coefficient. It is proved that no wind turbine generates more than 59.3 % kinetic energy of the wind into mechanical energy in order to rotate the mill. Conservation of mass and conservation of energy in a wind steam are the two approaches for fundamental theory of design and operation of wind turbines. The power coefficient of a wind turbine is related with Betz Limit Law from [**51**] & [**52**].

3.2.6. Air Density

Air density is another factor that affects wind power calculations. In order to calculate the density of air, elevation and temperature have to be accounted. Air pressure is the factor which affects density that depends on elevation from the sea level. Air pressure calculation is done using the basic approach to Pressure Theory. The derivation of Pressure Theory is based similarly on a subset of the International Standard Atmosphere (ISA) model, which is formulated by the International Civil Aviation Organization (ICAO). The relationship between Atmospheric pressure "p" and altitude "h" is indicated by [**53**]:

$$p = p_0 \left(1 - \frac{L.h}{T_0}\right)^{\frac{g.M}{R.L}} \approx p_0 . \exp\left(-\frac{g.M.h}{R.T_0}\right) \tag{41}$$

The formula extracted from equation (7) is:

$$p = 101325. (1 - (2.25577 \text{ x } 10^{-5}). h)^{5.25588} \tag{42}$$

According to the ideal gas law, it is:

$$\rho = \frac{P}{R_{specific} \cdot T} \tag{43}$$

where,

ρ = density of air (kg/m^3)
p = air pressure (Pa)
R = specific gas constant = 287.058 J/(kg.K)
T = absolute temperature (K)

According to [**2**], at sea level, standard temperature and pressure is 0 ^{o}C (273 K) and 101325 (Pa); the density of air is 1.2754 kg/m^3. Figure 21 and Figure 22 present monthly average air pressure and temperature measurement which were done using METU NCC wind tower measurement. The change in the pressure demonstrates that high temperature causes low pressure in the atmosphere; on the other hand, winter months have low temperature, meaning that there is a high pressure. Nevertheless, the variation in the pressure is too small; therefore, it can be taken as a fixed value.

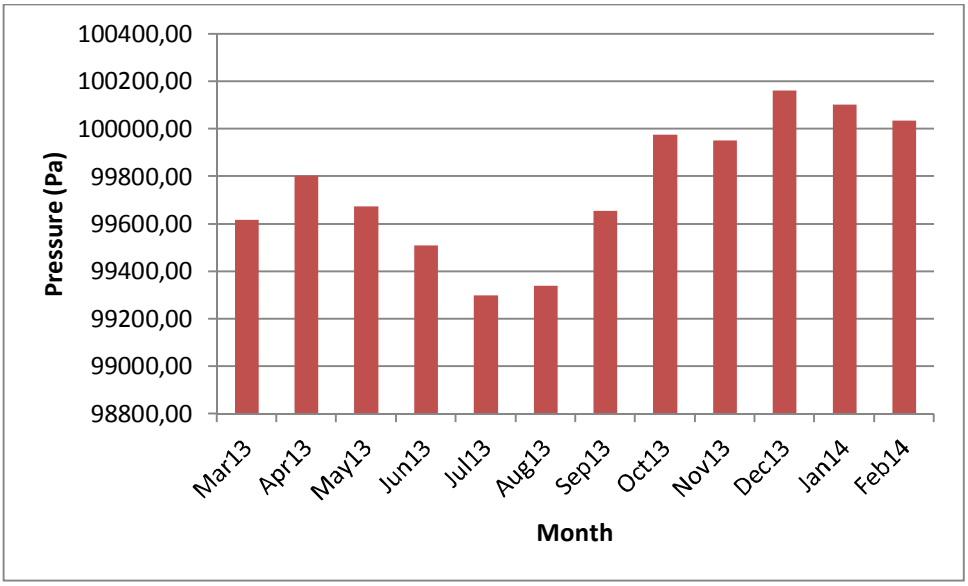

Figure 21: METU NCC Wind tower monthly average pressure

Figure 22 presents temperature variations of monthly averages of METU NCC. There is a reverse correlation between the temperature and air density. As temperature increases, air density decreases. The winter months have higher air density in comparison with the summer months; in addition to that it should be pointed out the pressure is higher in winter months.

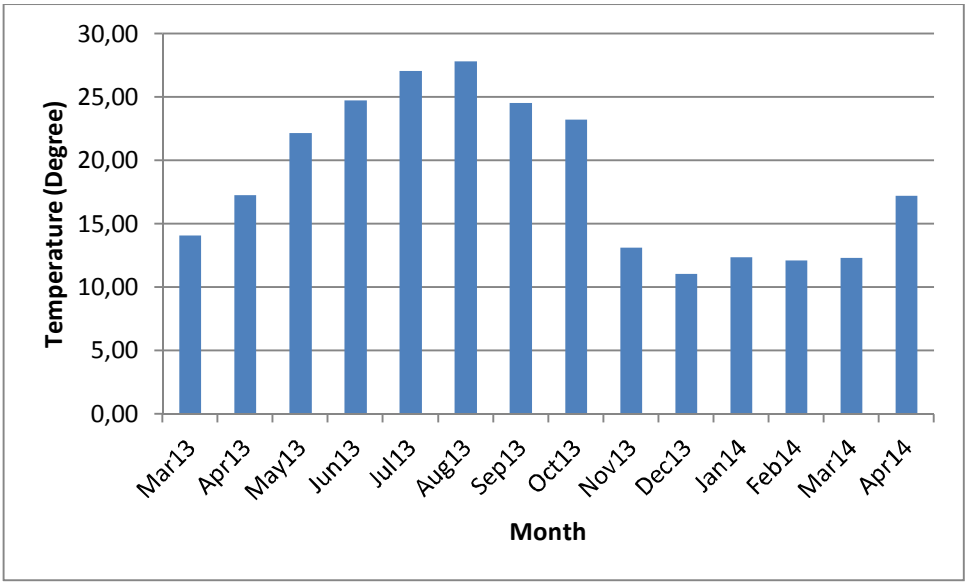

Figure 22: METU NCC Monthly average Temperature

3.2.7. Weibull Distribution

Weibull distribution is a probability density function in terms of wind speed and frequency and is widely used for wind energy analysis, life cycle cost, material properties, et cetera. Namely, it is a sort of analysis frequently used for stochastic processes. One of the most important advantages of Weibull analysis is the graphical plot of a sample data of an event occurring at a given time [**32**]. There are two main parameters; shape parameter and scale parameter. The formulation is presented as:

$$f(x;\lambda,k) = \frac{k}{\lambda}\left(\frac{x}{\lambda}\right)^{k-1} e^{-(x/\lambda)^k} \tag{44}$$

For Equation X, k > 0 is the shape parameter and $\lambda > 0$ is the scale parameter of the distribution. For a value of shape parameter k :

A value of k < 1 indicates that failure rate decreases over a period of time

A value of k = 1 indicates that failure rate is constant over a period of time

A value of k > 1 indicates that failure rate increases over a period of time

Linear Least Square Method, which calculates the k parameter of a formula, was used in order to find shape and scale parameter of Weibull distribution. To do this analysis, cumulative Weibull equation was modelled, which is demonstrated as:

$$F(v) = 1 - exp\left[-\left(\frac{v}{c}\right)^k\right] \tag{45}$$

$$\frac{1}{1-F(v)} = exp[\left(\frac{v}{c}\right)^k] \tag{46}$$

$F(v)$ is the cumulative Weibull distribution. The aim is that the formulation would be a linear line equation. Natural logarithmic of both sides were taken and it is indicated by the fact that:

$$ln\frac{1}{1-F(v)} = \left(\frac{v}{c}\right)^k \tag{47}$$

$$ln\,ln\frac{1}{1-F(v)} = k\,ln\,v - k\,ln\,c \tag{48}$$

Linear line equation is simply demonstrated as:

$$y = aX + b \tag{49}$$

Thus, the last thing is to decide the parameter of linear line equation to fit it with the equation derived.

$$y = ln\, ln \frac{1}{1-F(v)}\,, X = ln\, v\,, b = -k\, ln\, c\,, a = k \tag{50}$$

4. APPLICATION OF METHODOLOGY TO SOLAR ENERGY SYSTEM

4.1. Application of Methodology to Serhatköy PV Power Plant Dataset

As the PV module is verified with Serhatköy data in the previous section, the next step is to validate the PV model based on the same dataset.

Validation of the model is significant part of this research. Even though this model already exists in the literature, the aim is to compare the data and the model supports system compilation. In order to validate the model, Serhatköy PV farm solar irradiation data and energy output data are considered. Serhatköy PV farm involves 6192 of ANEL 205 NEC solar modules, 84 of 15 kW on-grid solar inverters. The total capacity of the system is 1.275 MW_P.

In Serhatköy, the panel angle is 25 degrees and the system measures solar irradiation on the same angle. Moreover, the temperature and electricity generation data are taken into account. In the analysis, global tilted solar irradiation data was used as the input of the model and the results are compared and contrasted as figures and tables. Following set of figures are the examples of the results of four specific days, i.e., spring and fall equinox, and summer and winter solstice. The yearly analysis and the errors of the module in comparison with the real-time measured data are presented in Table 8.

Consistent with the theory, the results are fitting with the real-time measured data with fewer errors for all years. The area underneath these shapes extracts the daily energy generation of applied PV system. By observing Figure 23 to Figure 26, there are slight differences between the real-time measurements and the PV model output.

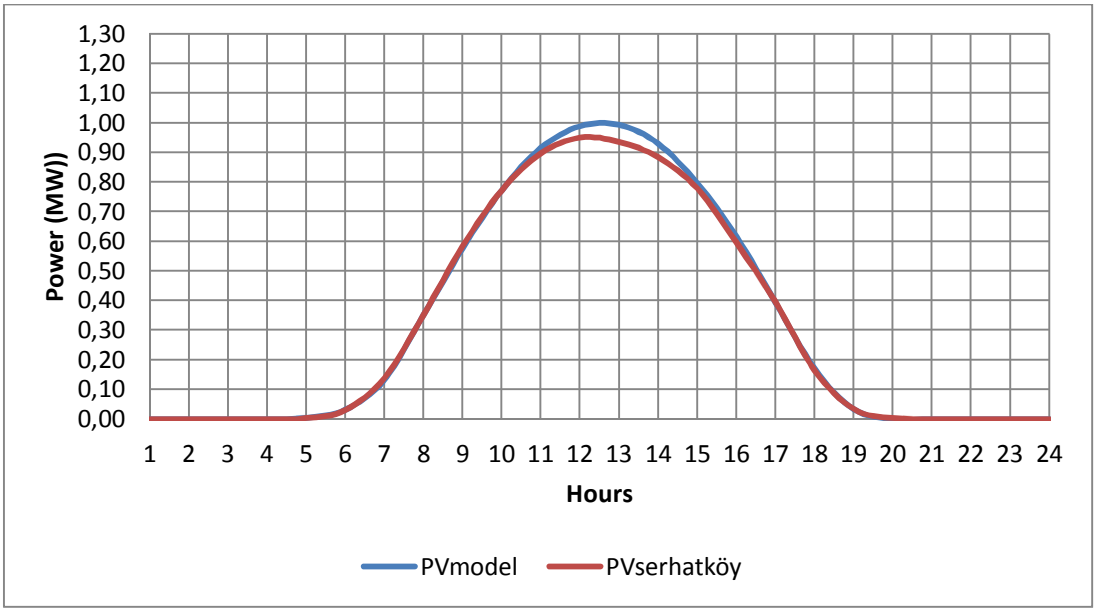

Figure 23: Serhatköy Electricity Generation vs PVmodel output in Summer Solstice, 21st June 2013

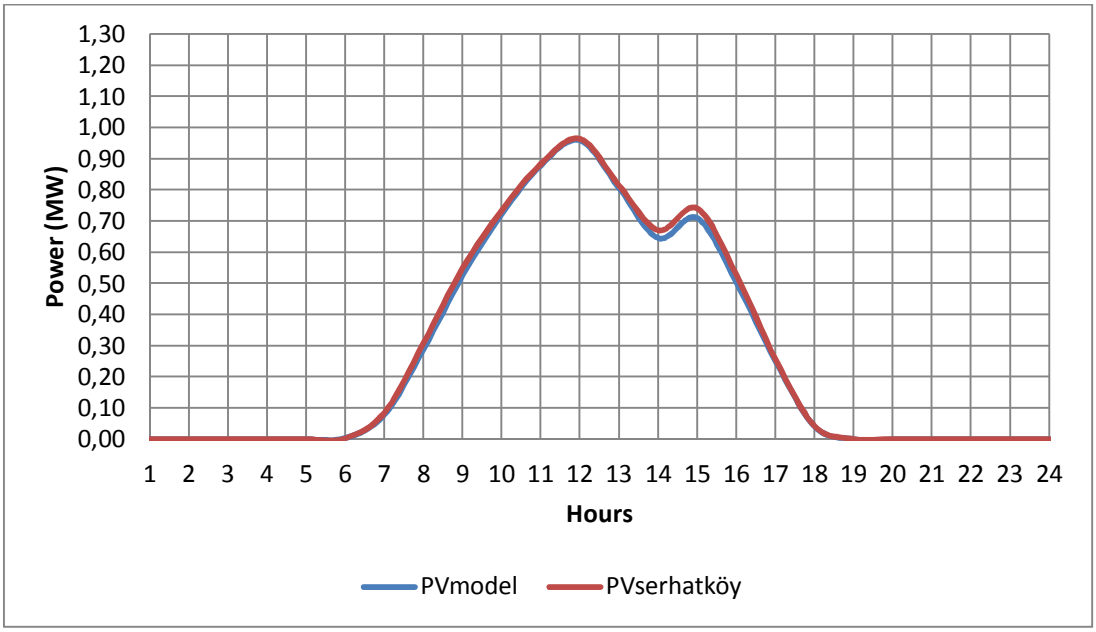

Figure 24: Serhatköy Electricity Generation vs PVmodel output in Fall Equinox, 21st September 2013

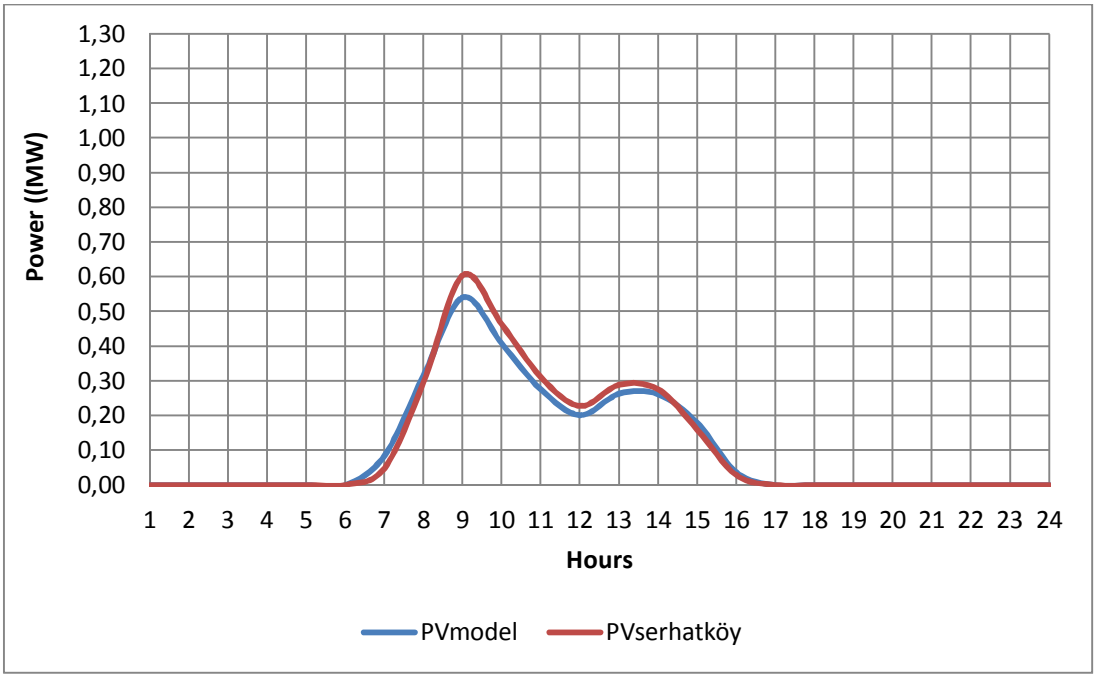

Figure 25: Serhatköy Electricity Generation vs PVmodel output in Winter Solstice, 21st December 2013

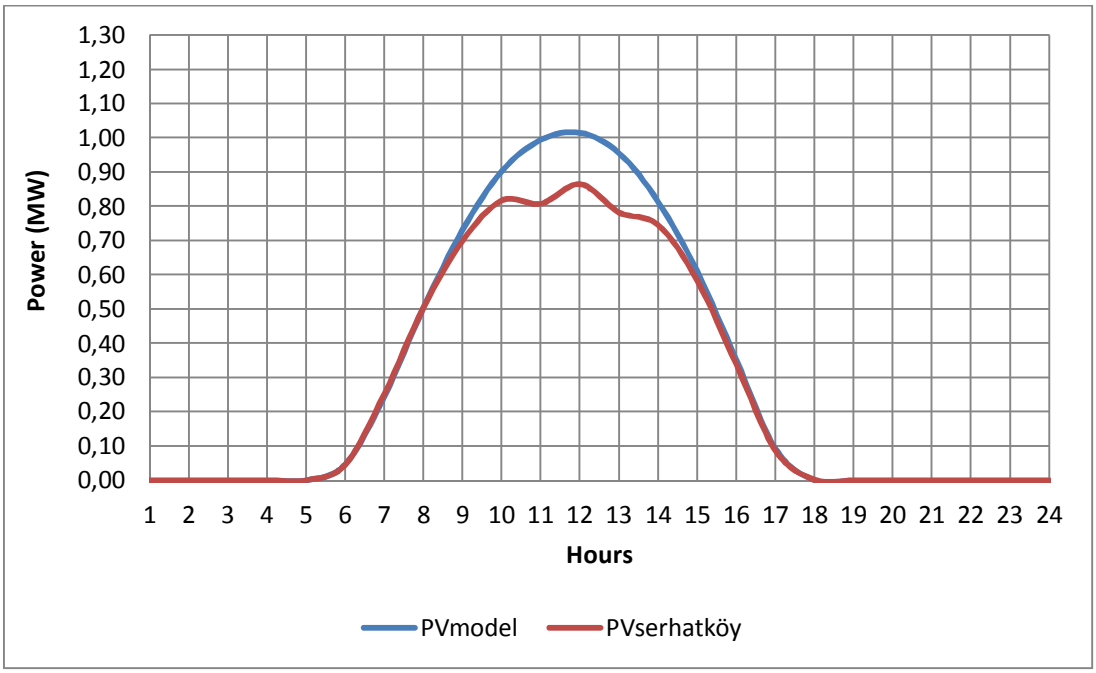

Figure 26: Serhatköy Electricity Generation vs PVmodel output in Fall Equinox, 21st March 2014

The system model works with Serhatköy PV data and the results are detailed in Table 8. Table 8 presents monthly total solar energy generation of PV model and the real-time measured solar energy PV output for Serhatköy measurements. Furthermore, the table demonstrates the solar fraction, which is defined as the solar energy conversion percentage from absorbed solar energy to electrical energy. Lastly, the monthly and yearly error percentages of model with respect to Serhatköy real-time measurements are illustrated.

The yearly total energy generation of PV model referring to the Table 8 is 2136 MWh; on the other hand, Serhatköy measurements illustrate that it is 2053 MWh. By looking at this point of view the error percentage of yearly energy generation is 3.89%. Error rates that are below 5 % are assumed to be reasonable for this work.

Table 8: Monthly Electricity Generation of Serhatköy PV Power Plant and presented PV model comparison

		PVmodel kWh	PVSerhatköy kWh	Fs PVmodel -	Fs PVserhatköy -	Error -
June13	6	212623.17	213637.01	11.19%	11.24%	-0.48%
July13	7	234809.61	229387.04	11.20%	10.94%	2.31%
August13	8	228949.63	209953.96	11.20%	10.27%	8.30%
Septemper13	9	199656.35	186170.84	11.19%	10.44%	6.75%
October13	10	184509.62	164340.65	11.18%	9.96%	10.93%
November13	11	120138.09	125593.77	11.17%	11.68%	-4.54%
December13	12	108658.04	116038.84	11.16%	11.92%	-6.79%
January14	1	119762.45	120925.61	11.16%	11.27%	-0.97%
February14	2	147357.18	160669.17	11.18%	12.19%	-9.03%
March14	3	183007.07	182284.19	11.14%	11.10%	0.39%
April14	4	197095.95	172443.16	11.18%	9.78%	12.51%
May14	5	200366.19	172389.55	11.19%	9.63%	13.96%
Annual		**2136933.35**	**2053833.80**	**11.18%**	**10.87%**	**3.89%**

Figure 27 illustrates the monthly total energy generation of a 1 kW_P system. It is important to note the normalized values due to small scale systems are more popular. The values are normalized to 1 kW_P. According to the Figure 27, the monthly total energy generation that is occurred in July; nevertheless, the day-time duration is higher in June. Through the June period, due to cloud activities, less day-time is observed. In comparison

with July, the day-time is higher but the total monthly energy generation is slightly less. To sum up, the yearly total energy generation of a 1 kW_P PV system is 1726 kWh.

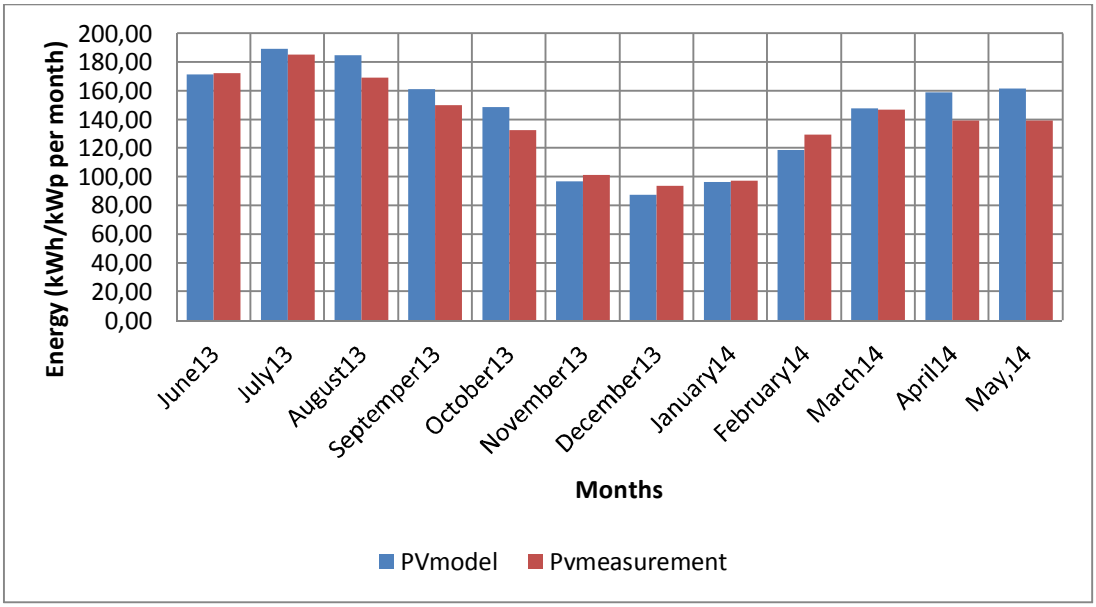

Figure 27: PVmodel vs Serhatköy Measurement normalized to 1 kW_p

A problem appears when Serhatköy solar irradiation and electricity generation data is examined. The problem is the system does not function through some of the days. Namely, the problem can be identified as there is solar irradiation data although there is not electricity generation. This problem occurs during the day-time. There are some possible reasons why this problem can occur. One scenario is it can be a maintenance issue during that time but there is not any log-book to check the maintenance issue. Another scenario is inverters can have a problem only for those periods. Among them, one of the most significant reasons, which have been identified, is the grid voltage harmonics. Harmonic is the corruption due to effect of non-linear load characteristic equipment can cause. This problem can be solved using harmonic filters and compensation systems. Unfortunately, Serhatköy PV farm compensation system does not function properly. Harmonics cause voltages corruption so that the inverters cannot generate the voltages. This problem was identified by the author using the log-book of the inverters.

As a result of above explanation, the problem causes increases in error observation. In order to pull the error back to a more reasonable level, and to be able to interpret the problematic data with more realistic ones, a hypothesis is developed. The first part of

applying the hypothesis is defining and finding the not-working hours of PV plant. Secondly if the hours are known, the possible energy generation can be found using the presented PV model because the error percentage of the model is reasonable. Lastly, addition of the found not-working hours to the real-time measurement of the plant can extract the approximate real estimation of the PV power plant. The results are indicated in Table 9.

Table 9: PV plant not functioning hours and energy generation for presented model

	Month	PVserhatköy not working kWh	PVmodel	PVserhatköy	
June13	6	1807.05	212623.17	215444.07	-1.33%
July13	7	0.00	234809.61	229387.04	2.31%
August13	8	136.14	228949.63	210090.10	8.24%
Septemper13	9	9931.73	199656.35	196102.57	1.78%
October13	10	25175.08	184509.62	189515.73	-2.71%
November13	11	1771.94	120138.09	127365.70	-6.02%
December13	12	651.74	108658.04	116690.58	-7.39%
January14	1	6980.65	119762.45	127906.26	-6.80%
February14	2	0.00	147357.18	160669.17	-9.03%
March14	3	892.83	183007.07	183177.02	-0.09%
April14	4	24884.03	197095.95	197327.18	-0.12%
May14	5	24007.33	200366.19	196396.88	1.98%
Annual		**96238.52**	**2136933.35**	**2150072.31**	**-0.61%**

Table 9 illustrates the result of monthly total non-functioning hours of the PV power plant electricity generation using presented PV model. PV Serhatköy represents Serhatköy PV plant measured production in addition with the not-working hour's energy generation. As a result of this analysis, the yearly energy generation of Serhatköy power plant and the PV model output fits well to each other. Accordingly, the error rate decreases to 0.61%. Since it is an already-existed circuit based PV model, one of the important aspects of this hypothesis is to reveal the model accuracy. It is summarized from the model validation that the model works with less than 1% error. Moreover, PV model can be used for identifying non-working hours and also finding the electricity generation for those hours.

4.2. GTI Calculation Using METU NCC DNI and GHI dataset

Using the above equations, Serhatköy GTI prediction was done and it is presented in Table 10. Referring to the Table 10, one year period of the data was starting from June 2013 to May 2014. Although October 2013, April 2014 and May 2014 data have problems, they were taking into account due to obtain a complete year of dataset. To note some of the important aspects of this analysis, the error percentage of a year is found as 2.37%, which is less than 5 percent; therefore, this analysis is reasonable. Moreover, allocating the months, which have erroneous measurements, the error percentage is going to be changed.

Table 10: GTI prediction results using METU NCC GHI and DNI measurement

		METU NCC kWh/m2	Serhatköy kWh/m2	Error
June13	6	248.97	205.59	17.42%
July13	7	257.91	226.95	12.00%
August13	8	233.49	221.27	5.23%
Septemper13	9	203.79	193.05	5.27%
October13	10	204.53	178.50	12.73%
November13	11	112.16	116.26	-3.66%
December13	12	100.92	105.25	-4.28%
January14	1	109.32	115.98	-6.09%
February14	2	150.39	142.68	5.12%
March14	3	184.17	177.77	3.47%
April14	4	169.94	190.73	-12.23%
May14	5	142.55	193.83	-35.97%
Annual		**2118.14**	**2067.85**	**2.37%**

4.3. Serhatköy PV Power Plant Electrical Energy Production Using METU NCC Solar Irradiation Dataset

METU NCC measurement station GHI and DNI data are used to generate and predict GTI values of Serhatköy measurements for each hour of a year. Including the PV model analysis to estimate GTI data, the Serhatköy PV farm was predicted with the error of 4.74%. (Refer to Table 10). The yearly energy generation of the plant was calculated as 2156 MWh; however, the actual production is 2053 MWh. To note one of the important

points into this analysis, the Serhatköy non-working hours were not involved. Referring to Table 9, the actual energy generation is about 2150 MWh so that the prediction error was decreased.

Table 11: Serhatköy PV Power Plant production using METU NCC GTI solar irradiation data

		PVmodel kWh	PVSerhatköy kWh	Error
June13	6	244322.03	213637.01	12.56%
July13	7	237394.71	229387.04	3.37%
August13	8	207734.79	209953.96	1.06%
Septemper13	9	200150.92	186170.84	6.98%
October13	10	218886.01	164340.65	24.92%
November13	11	117079.36	125593.77	6.78%
December13	12	113274.88	116038.84	2.38%
January14	1	121623.32	120925.61	0.57%
February14	2	170152.84	160669.17	5.57%
March14	3	206193.54	182284.19	11.60%
April14	4	181457.93	172443.16	4.97%
May,14	5	137868.72	172389.55	20.02%
Annual		**2156139.05**	**2053833.79**	**4.74%**

To note some of the aspects of this analysis, the results are promising in comparison with the real measurements at Serhatköy. It is also necessary to find out where the Northwestern Cyprus potential and the energy generation capacity factor. In order to find the capacity factor of Serhatköy, the actual generation is divided by the potential energy generation (assuming 24 hour, 365 days of maximum power full capacity production). Equation (51) presents capacity factor of PV model results for Serhatköy energy generation from June 2013 to May 2014), which is 19.38 %. Whereas, the same equation is used with the actual measured energy generation, and the result decreased to 18.45%, and it is illustrated in Equation (52).

$$\frac{2156\ MWh}{1.27 MW_p x\ 8760\ h} = 19.38 \tag{51}$$

$$\frac{2053\ MWh}{1.27 MW_p x\ 8760\ h} = 18.45 \quad (52)$$

Referring to Table 9, there is 96 MWh of energy generation which Serhatköy PV plant did not produce due to technical problems in the electrical grid. This is observed and illustrated by using the PV model. In fact, almost 4% of the energy generation of Serhatköy is wasted due to these reasons. Therefore, the actual energy generation of Serhatköy can be calculated by adding 96 MWh energy to the actual measurements; thus, 2149 MWh energy can be produced. As a result of this analysis, the capacity factor found in the Equation (51) is more accurate than the actual measurement.

Comparison of Serhatköy PV plant results with other regions in the world extracts the solar energy potential of Northwestern Cyprus with respect to actual measurements. A well-rounded [**54**] study has been done to carry out solar energy potential of Turkey. The regional total global horizontal solar irradiation and sunshine duration hours are presented in Table 12. Table 12 demonstrates that topographic factor plays a significant role in solar energy absorption and values are found between 1305 and 1648 kWh/m^2. Thus the most dominant area, which has higher solar irradiation with respect to others, is found as Southern Anatolia, whereas, the least one is the Black Sea and other regions are between them. In Northwestern Cyprus, the total GHI and DNI solar irradiation observed are 1886 and 2035 kWh/m^2 respectively. In consequence, in the light of the METU NCC measurement data, Northwestern Cyprus has higher solar irradiation in comparison with Turkey regional average. Total energy generation using PV model is calculated as 2156 MWh although energy generation of the best energy absorption area, Southern Anatolia, is 1700 MWh (if 1.27 MW$_p$ power plant with the same devices is applied). Moreover, a Serhatköy real-time measurement supports this finding as well.

*Table 12: Regional total global horizontal solar energy potential and sunshine duration hours in Turkey [**54**] and 1.27 MW_p PV plant energy generation*

Region	Total Solar Energy kWh/m2	Sunlight Hour hour/year	1.27 MWp PV MWh
Southern Anatolia	1648	2845	1700
Mediterranean	1548	2737	1597
Aegean	1528	2615	1576
East Anatolia	1523	2519	1571
Inland Anatolia	1481	2563	1528
Marmara	1329	2250	1371
Black Sea	1305	1929	1346

To compare the results, the two leading country in terms of installed capacity of PV is considered in this study. Solar irradiation measurement in 2013 of Almeria (Spain), Stuttgart (Germany) and METU NCC (Northwestern Cyprus) are presented in Figure 28. Germany is European leader and Spain is the second in terms of installed capacity of PV [**15**] [**55**]. Although Almeria results are promising in terms of solar irradiation absorption, METU NCC measurements indicate that Northwestern Cyprus is the better than Spain. To compare the results with Germany, capacity factor of Northwestern Cyprus is approximately twice of the Germany.

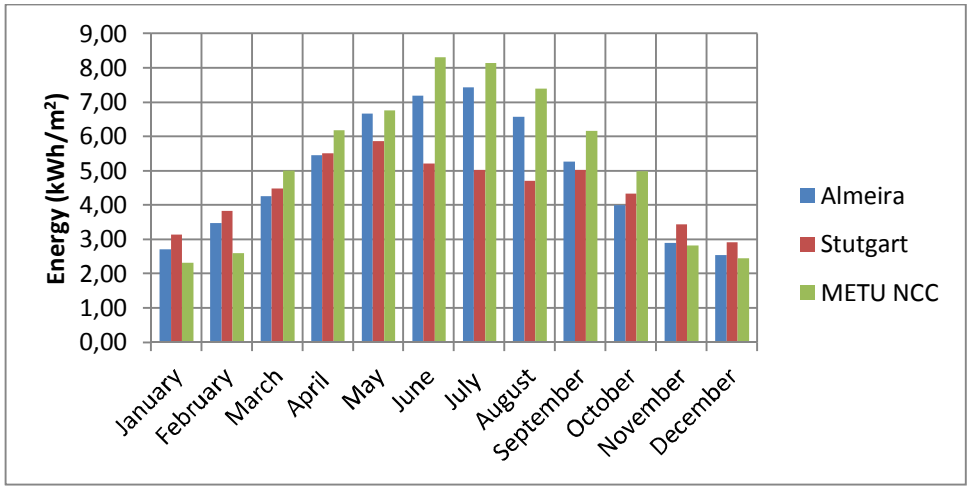

*Figure 28: Average monthly global horizontal solar irradiation measurements in Almeria, Stuttgart and MET U NCC in 2013 [**55**]*

5. APPLICATION OF METHODOLOGY TO WIND ENERGY SYSTEM

5.1. Weibull Distribution of Wind dataset

For METU NCC wind tower, 30th, 50th and 60th meters were analyzed as 40th meter had a problem at some time during the data collection so that it was not taken into account since a full year data could not be collected. Applying the model derived for Weibull analysis, the real-time measurements can be indicated as:

30th meter Weibull characteristics: k = 1.74 and c = 4.49

50th meter Weibull characteristics: k = 1.75 and c = 4.94

60th meter Weibull characteristics: k = 1.74 and c = 5.16

Once the Weibull characteristics were calculated, the best fit Weibull graph with the Weibull analysis are indicated in Figure 29, Figure 30 and Figure 31 for 30th, 50th, and 60th meters of the wind tower respectively.

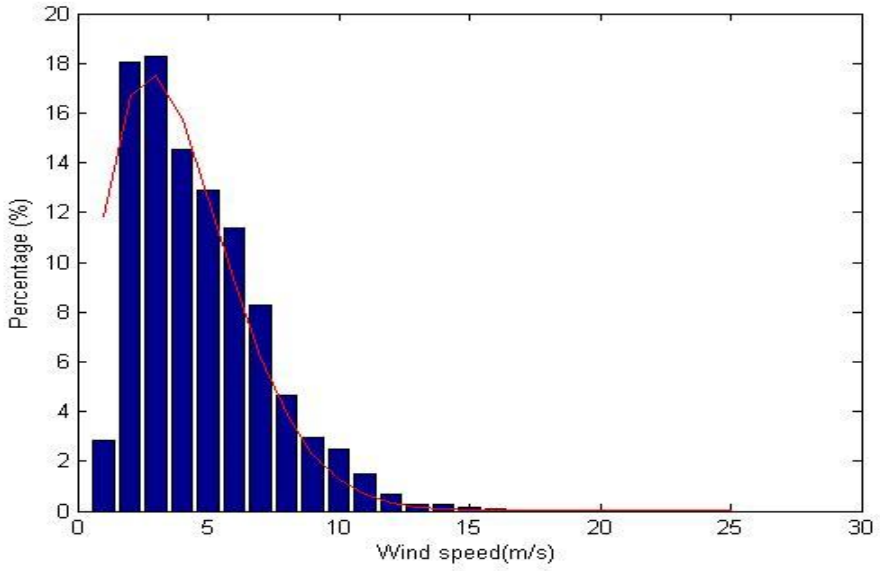

Figure 29: 30m weibull analysis

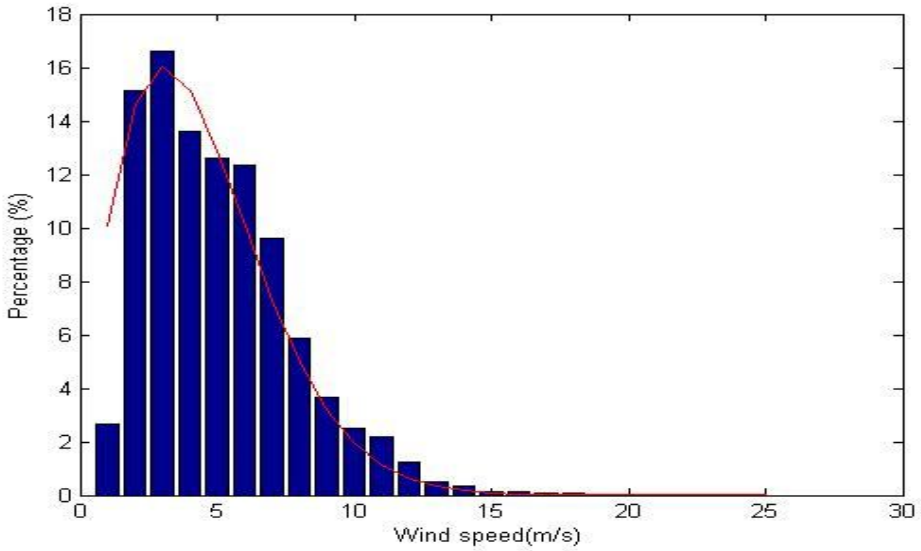

Figure 30: 50m weibull analysis

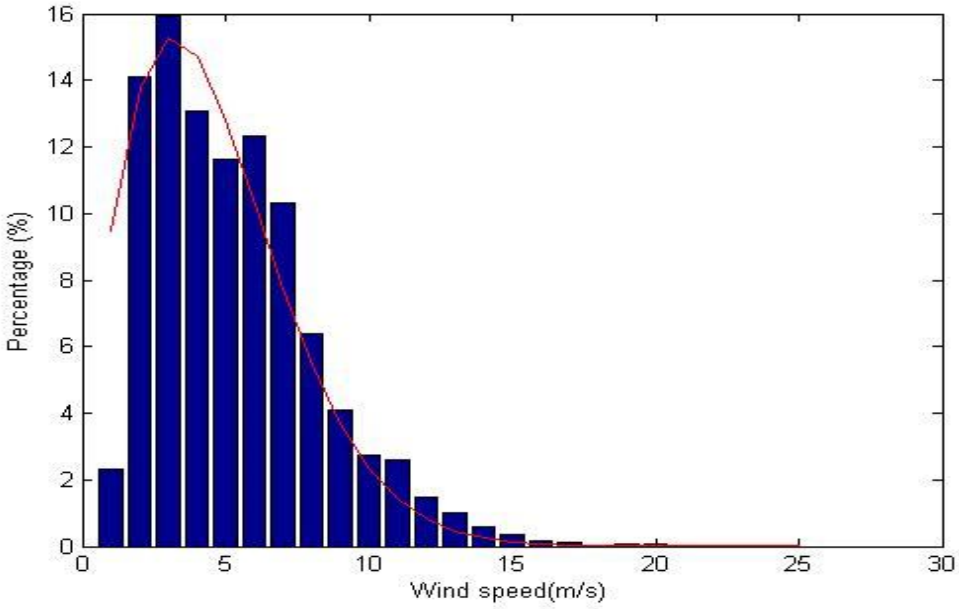

Figure 31: 60m weibull analysis

5.2. Electrical Energy Generation

It is a matter of common observation that the wind speed is not steady, and in order to calculate the mean power delivered by a wind turbine from its power curve, it is necessary to know the probability density distribution of the wind speed. To be more specific, this is the distribution of the proportion of time spent by the wind within narrow bands of wind speed.

In order to analyze the energy generation three separate wind speeds, which are 30^{th}, 50^{th} and 60^{th} meter of the tower, are used. Vestas wind towers were also used for this analysis. Vestas V27, Vestas V47, Vestas V66 are the types of devices, which are apparently used for the analysis of wind energy generation. Table 13 indicates specifications of Vestas devices used in this thesis.

*Table 13: Vestas wind tower specifications [**56**] [**57**]*

	Vestas		
	V27	V47	V66
Swept Area (m^2)	572	1735	3421
Cut in Speed (m/s)	3.5	4	4
Cut out Speed (m/s)	16	16	16
Rated Speed (m/s)	25	25	25
Rotor Diameter (m)	27	47	66
Hub Height (m)	31	50	60
Rated Power (kW)	225	660	1650

The results of electricity generation prediction for four specific days are presented in Figure 32 to Figure 35. The model validation is not done for this research due to the lack of output energy generation data near around Northwest Cyprus. Thus the model is taken from the literature. Many research about this area have been carried out to find the energy

generation equation, i.e., Equation (40). To note some of the important aspect of this analysis by observing Figure 32 -Figure 35, wind is a variable resource. In Figure 32, for instance, there is no electricity generation up to 6th hour. Nevertheless, the electricity generation reaches to pick values at the hour of 22:00 for 50th and 60th meter of the tower measurements. This means that the wind speed is higher than the rated or equal to the rated speed of the turbine characteristic. On the other hand, the electricity generation for the days of 21st of June 2013 is on the average level since the month is a summer month. Nonetheless, there is practically not any electricity generation on 21st of December 2013. Although the month is a winter month, the electricity generation variable depends mostly on the wind speed factor.

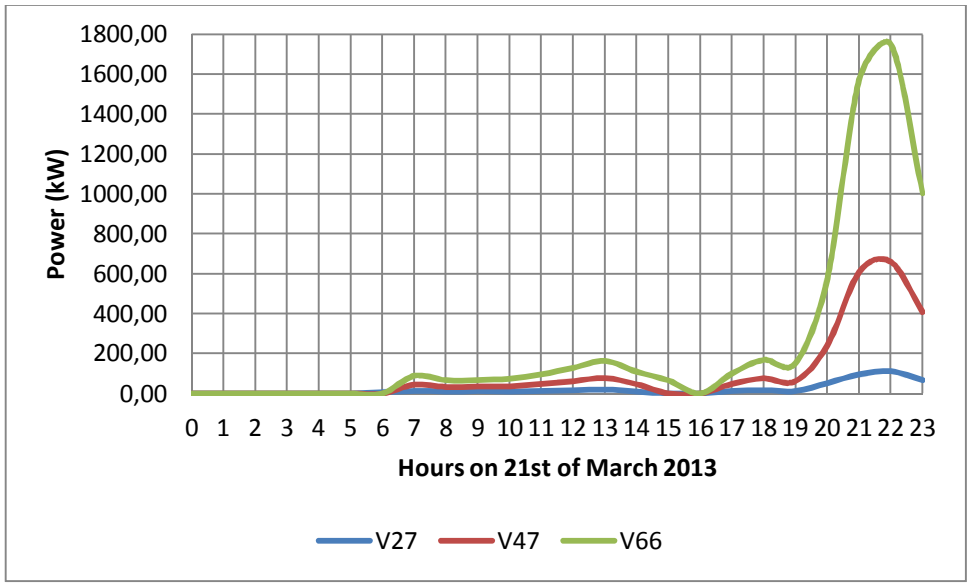

Figure 32: Vestas V27, V47, V66 electricity generation prediction model output on 21st of March 2013

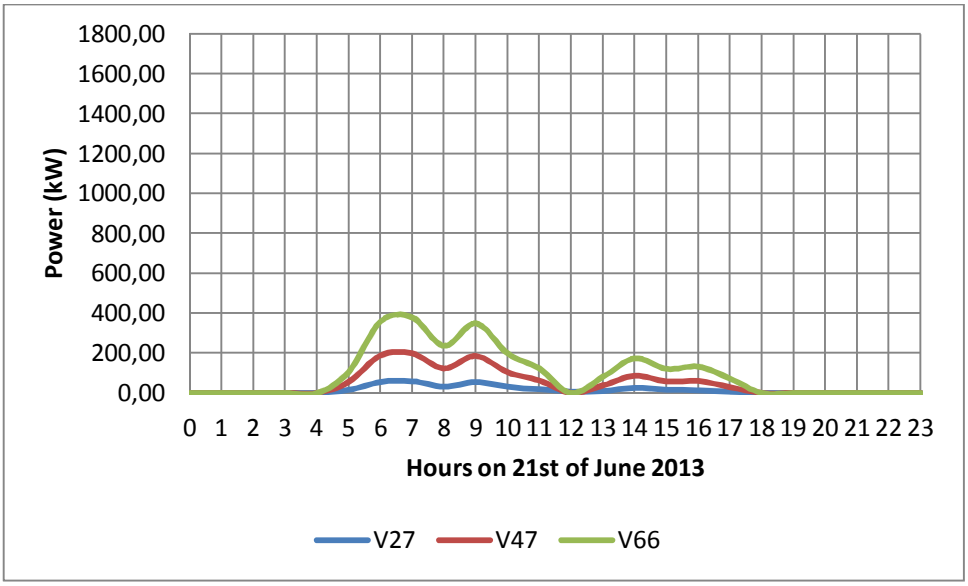

Figure 33: Vestas V27, V47, V66 electricity generation prediction model output on 21st of June 2013

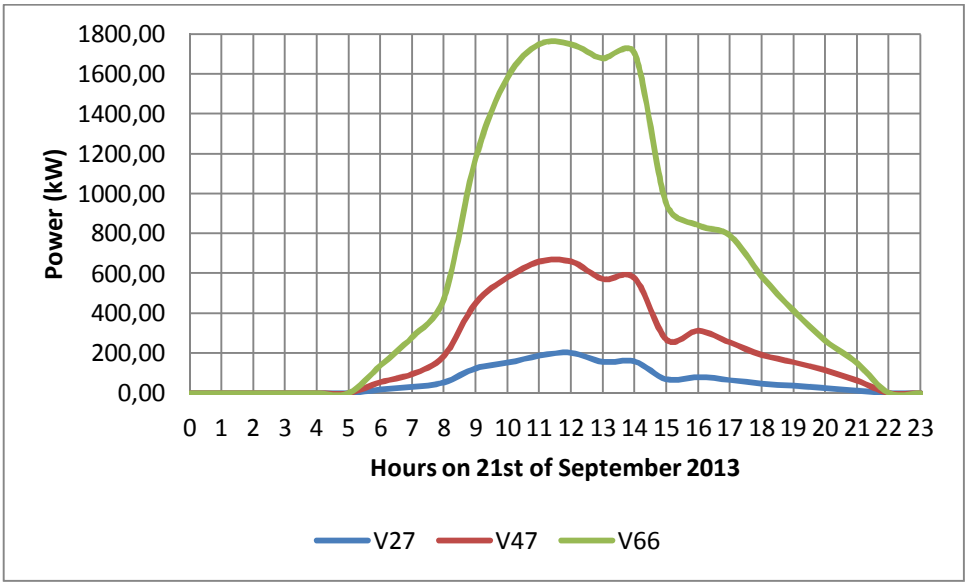

Figure 34: Vestas V27, V47, V66 electricity generation prediction model output on 21st of September 2013

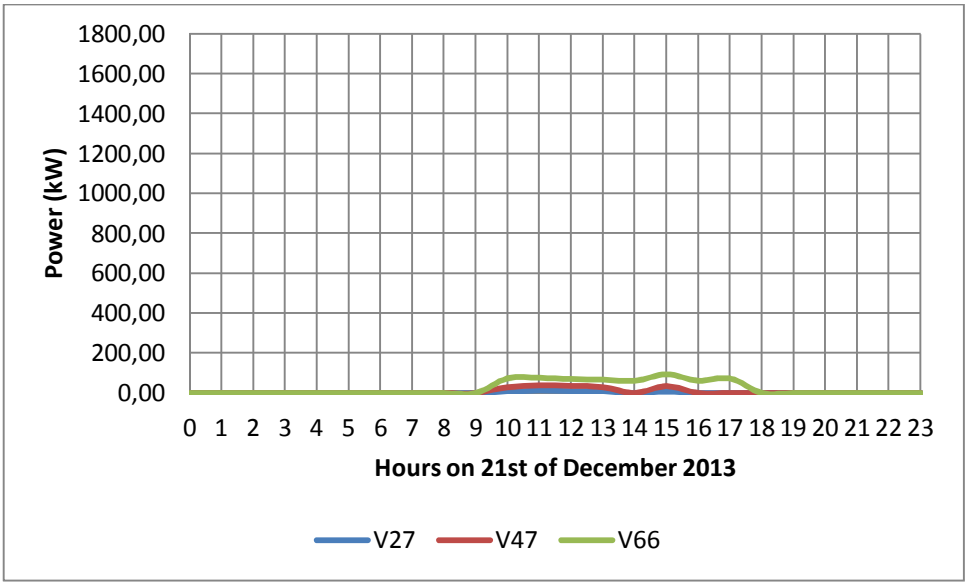

Figure 35: Vestas V27, V47, V66 electricity generation prediction model output on 21st of December 2013

Table 14: Monthly and yearly total electricity generation of Vestas V27, V47 and V66.

	Vestas V27 MWh	Vestas V47 MWh	Vestas V66 MWh
March 2013	31.18	114.92	287.87
April 2013	18.96	68.73	169.38
May 2013	11.99	44.54	107.91
June 2013	18.41	69.09	170.72
July 2013	10.05	36.65	85.98
August 2013	9.86	36.53	86.54
September 2013	14.32	53.29	133.43
October 2013	12.33	45.22	108.82
November 2013	10.61	43.70	105.36
December 2013	21.00	75.90	179.75
January 2014	9.80	40.23	96.72
February 2014	8.48	32.85	74.84
Yearly Total Electricity Generation	**177.00**	**661.65**	**1607.34**

Table 14 presents electricity generation prediction of Vestas V27, V47 and V66 as 177.00, 661.65 and 1607.34 respectively. According to Table 14, Vestas V27 has thirty-one

meters hub height; therefore, thirty meter wind speed was used in order to get energy. The tower generates 177 MWh energy during the given period. Capacity factors of the turbines are described as yearly total energy generation divided by the maximum yearly total energy generation. Namely, it is the value that gives the average total energy generation for presented wind power plant. Annual electricity generation and capacity factor of the Vestas V27, V47 and V66 wind power plants are indicated in Table 15. Referring to Table 15, the capacity factors of selected wind turbines are 8.98, 11.44 and 11.12 respectively.

To sum up, the information taken from existed mathematical model indicates that capacity factor of Vestas V27, V47 and V66 is lower than 20 % value so that installing these wind turbines are not feasible for Northwest Cyprus. The large scale wind turbines can be in a feasible range to apply wind energy on METU NCC which is indicated by the fact that hub height is higher than 60 meter of the wind turbines which is the significant and valuable demonstration of the model. However, higher than 60 meter of the wind speed were not measured/analyzed.

It is concluded that the wind is a viable renewable resource, yet it is not feasible due to the effect of capacity factor for the location. The results also indicate that the effect of electricity generation increases depending on the height. For instance, V27 and V66 generated 177 and 1607 MWh electricity respectively. The summary demonstrates that the 30 meter increase in height with respect to 30 m hub height V27 may increase output electricity generation about 8 times. Lastly, it is not possible to compare the energy generation data of the model since there is not any wind power plant in the North-West part of the island. However, the presented model in the methodology part is an already-existed model so that the validation part may not be regarded as necessary.

Table 15: Capacity factor of presented wind turbines with different heights

	Vestas		
	V27	**V47**	**V66**
Swept Area (m^2)	572.26	1735	3421
Cut in Speed (m/s)	3.5	4	4
Rated Speed (m/s)	16	16	16
Cut out Speed (m/s)	25	25	25
Rotor Diameter (m)	27	47	66
Hub Height (m)	31	50	60
Rated Power (kW)	225	660	1650
Energy (MWh)	177.00	661.65	1607.34
Capacity Factor	8.98%	11.44%	11.12%

Wind energy analysis is done with the data gathered from METU NCC wind tower. Since wind power is a type of renewable energy, it might provide an attractive solution for the future energy problem. Southern Cyprus has made an important attempt to reach European Union's renewable energy target by 2020 [**58**]. The state-owned Electricity Authority of Cyprus has to buy 113.5 megawatts of energy from two new operators, Orites wind farm in Paphos and Ketonis wind farm in Larnaca. Nowadays, 144.3 MW installed capacity of wind energy have been supporting the electricity grid. The average monthly electricity generation of wind farms of Southern Cyprus in 2013 illustrated in According to **Error! Not a valid bookmark self-reference.**, capacity factor of the wind turbines are slightly high in comparison with presented model output. As it is presented in this thesis, topographical characteristic of a field affect the electricity generation of wind turbines. A comprehensive study has been done to summarize the installed cost, capital cost, average capacity factor and O&M cost of wind turbines for different regions over the world , and they are presented in Table 17. Referring to Table 17, capacity factor of Northwestern Cyprus is below the world average; whereas, it is almost equal to the Southern Cyprus.

Table 16.

According to **Error! Not a valid bookmark self-reference.**, capacity factor of the wind turbines are slightly high in comparison with presented model output. As it is presented in this thesis, topographical characteristic of a field affect the electricity generation of wind turbines. A comprehensive study has been done to summarize the installed cost, capital cost, average capacity factor and O&M cost of wind turbines for different regions over the world [**60**], and they are presented in Table 17. Referring to Table 17, capacity factor of Northwestern Cyprus is below the world average; whereas, it is almost equal to the Southern Cyprus.

*Table 16: Monthly electricity generation and capacity factor of wind Turbines in 2013 [**59**]*

	Installed Capacity MW	Monthly Electricity Generation MWh	Capacity Factor -
January 2013	144.3	15455.11	14.396%
February 2013	144.3	14321.66	14.769%
March 2013	144.3	18802.37	17.514%
April 2013	144.3	13408.56	12.906%
May13	144.3	11242.58	10.472%
June 2013	144.3	14512.32	13.968%
July 2013	144.3	13130.86	12.231%
August 2013	144.3	11807.28	10.998%
September 2013	144.3	10941.12	10.531%
October 2013	144.3	13911.31	12.958%
November 2013	144.3	9693.36	9.330%
December 2013	144.3	19223.47	17.906%
Annual		**166450.01**	**13.165%**

*Table 17: Summarization of Wind Turbine cost and capacity factor [**60**]*

	Installed Cost (2010 $/kWh)	**Capacity Factor (%)**	**O&M ($/kWh)**
Onshore			
China/India	1300 to 1450	20 to 30	n.a
Europe	1850 to 2100	25 to 35	0.013 to 0.025
Northern America	2000 to 2200	30 to 45	0.005 to 0.015
Offshore			
Europe	4000 to 4500	40 to 50	0.027 to 0.048

6. CONCLUSION AND FUTURE WORK

6.1. Conclusion

As explained in detail in the introduction section, sustainable energy systems may be the solution for future electricity problems. Among all renewable resources, solar and wind energy systems are the most promising ones due to the decline in associated costs of these technologies. A methodology is organized to calculate the electrical energy production based on the hourly solar resources and wind resources. This methodology can be applied to similar assessments in different regions. Considering a good solar resource potential in Northwestern Cyprus, a higher capacity solar PV power plant can be installed or Serhatköy plant capacity can be increased. On the other hand, wind energy results demonstrates that the capacity factor of the wind is below the world average.

An already existing model for PV type solar energy in the literature is used in the methodology section, of which also addresses solar irradiation measurements. The first part of applying methodology is examining the solar data. The analysis defined in this part consists of estimating electricity generation and the efficiency of the PV panels with respect to meteorological conditions, and calculating the capacity factor of an installed PV system. There are several methods to model the link between measured solar irradiation and electricity generation. Circuit-based single diode model was used and first applied in Serhatköy PV power plant. It is done to validate the model accuracy and the validation indicated that the error is less than 1 %, the accuracy of the model is promising. Namely, the model yields that results are in good agreement with the measured data at Serhatköy.

The data taken from METU NCC measurement station involves global horizontal and direct normal solar irradiation. In order for the control of the data, clear sky model found in the literature was used. The data seems to be without major problems starting from July 2013 till March 2014. However, from April 2014 till October 2014, there are some problems with the measurements such that the data was measured seemed to be approximately half of the previous year's values. Therefore, the best option is to use the data starting from June 2013 till May 2014. With this, the measured solar resource data for the entire year was predicted and used in the thesis.

Using METU NCC GHI and DNI data, an entire year of global tilted solar irradiation was calculated. The data was compared with the measured dataset in Serhatköy, which noted that Serhatköy measurement is global tilted solar irradiation. Analysis results illustrated that the calculation results assumed to be reasonable since the error is less than 5 %. Applying the presented PV model, Serhatköy electrical energy production was calculated using METU NCC GHI and DNI data. The model outcome indicated that the Serhatköy electrical energy generation was calculated as 2156 MWh, but the actual measurement in Serhatköy is 2053 MWh. With this, the error is 4.77%. However there are some problems in Serhatköy plant energy production due to technical problems and human error (at times of certain electrical outages of the grid, the PV plant was disconnected but not reconnected after the problem was fixed, due to operator negligence). The other problem is the fact that inverters do not function properly due to the improper system voltage at times, which was due to the compensation system not working properly. It was concluded that the error of the electrical energy production using METU NCC measurement could be less if the defined problems were fixed. It was also concluded that estimating electricity generation of Serhatköy PV plant using METU NCC measurements are reasonable in accuracy; with this type of tool METU NCC measurements can predict PV plant production with reasonable accuracy for any specific location in Northwestern Cyprus.

While observing the PV capacity of Northwestern Cyprus, the wind energy analysis can be added to support the system. Wind energy is a viable resource like solar energy but for this region it is below world standards. This is due to the fact that the wind speed has a cubic factor dependence for electricity generation and it can vary significantly for different topographies, even in close by areas. METU NCC wind tower results are considered for this analysis. There are four anemometers our wind tower to measure wind speed with different heights; which are 30^{th}, 40^{th}, 50^{th}, and 60^{th} meters. 40^{th} meter anemometer was not functioning for some periods so it was extracted from the dataset.

In order to check the measured data, data correlation between the levels of measurement were done. In the methodology and throughout the whole thesis, it was also underlined that the measurements would be reasonably accurate. The correlation analysis was done to check whether the 30^{th}, 50^{th} and 60^{th} meter measurements are correct. The results of this analysis illustrated that the dataset seemed to have good correlation for throughout the year. There is some other observation station in Northwestern Cyprus;

nevertheless, they did not share their dataset. Hence the measurements were not compared with other stations.

After the checking the measurements, a clear methodology from literature was applied in order to calculate electrical energy production using wind measurements. The methodology for this part is general in application and can be applied to different regions, if similar inputs in the dataset is available. The hourly average wind speed, temperature, humidity and air pressure are required for the methodology, the results illustrated the electrical energy production for the wind energy system. To obtain the energy output Vestas V27, V47 and V66 models were selected for 30^{th}, 50^{th} and 60^{th} meters of wind speed measurements. The validation of the model was not done due to the fact that the model is used in many other studies. The results of the model demonstrated that the capacity factor of 30^{th}, 50^{th} and 60^{th} meter turbines are 8.98%, 11.44% and 11.12% respectively. It was concluded that the wind energy capacity for the Northwestern part of the island is below the world average. It also showed that the wind capacity factor in this region is even less than a solar PV system (which is not usually the case). Therefore, it was also concluded that there is a high solar energy potential but the wind capacity is not as expected. Using the tools developed for this thesis similar assessments can be made for different regions.

6.2. Future Work

In this work, the designing of PV system and wind energy system is investigated and explored. Future work in this area may include any tracking surfaces, i.e., East-West tracking, North-South tracking and 2-axis tracking. Future work may also include economic assessment of both solar energy system and wind energy system. Storage options of PV or Wind energy system are not considered; therefore, any backup system may include for future research. Despite the fact that the wind profile of Northwestern Cyprus is not promising, a more comprehensive study for wind rose height-wind speed relationship would contribute to a better understanding of its potential. The orientation analysis may also be added to this methodology to find out the best tilt angle in Northwestern Cyprus.

REFERENCES

[1] E., Njomo, D. Mboumboue, "Mathematical modeling and digital simulation of PV solar panel using MATLAB software," *International Journal of Emerging Technology and Advanced Engineering*, vol. 3, no. 9, pp. 24-32, September 2013.

[2] J. W., DRAKE, E. M., DRISCOLL, M. J., GOLAY, M. W., & PETERS, W. A. TESTER, *Sustainable energy: Choosing among options*.: MIT, 2005.

[3] (2014, May) British Petrol. [Online]. www.bp.com

[4] S. V. Valentine, "The socio-political economy of electricity generation in China," *Renewable and Sustainable Energy Reviews*, vol. 32, pp. 416-429, 2014.

[5] A.J., Szabo, M., Scarlat, N., Ferrario, F.M. Waldau, "Renewable electricity in Europa," *Renewable and Sustainable Energy Reviews*, vol. 15, pp. 3703-3716, 2011.

[6] E., Medvedev, A., Hooper, "Electrifying integration: Electricity production and the South East Europe regional energy market," *Utilities Policy*, vol. 17, pp. 24-33, 2009.

[7] International Energy Agency, "World Energy Outlook 2013," 2013.

[8] X.X., Lin, Y.G., Li, W., Liu, H., Gu, Y., Yin, "Output power control for hyrdo-viscous transmission based continuously variable speed wind turbine," *Renewable Energy*, vol. 72, pp. 295-405, 2014.

[9] E., Khan, "Reliability of distributed wind generators," *Electric Power System Research*, vol. 2, pp. 1-14, 1979.

[10] Holttinen H., "Hourly wind power variations in the Nordic Countries," *Wind Energy*, vol. 8, no. 2, pp. 173-195, 2005.

[11] G., Sinden, "Characteristics of the UK wind source: long-term patterns and relationship to electricity demand," *Energy Policy*, vol. 35, no. 1, pp. 112-27, 2007.

[12] Y., Chan, L.C., Shu, L., Tsui, K., Su, "Real-time prediction models for output power and efficiency of grid-connected solar photovoltaic systems," *Applied Energy*, vol. 93, pp. 319-326, 2012.

[13] Y.V., Sachenko, A.V., Bobyl, A.V., Kostylyyov, V.P., Sokolovskyi, I.O., Terukov, E.I., Tokmoldin, N., Tokmoldin, S. Zh., Smirnov, A.V., Kryuchenko, "Evaluation of

the annual electric energy output of an A-Si:H solar cell in various regions of the CIS countries," *Energy Policy*, vol. 68, pp. 116-122, 2014.

[14] "Global trend in wind power with special focus on top five wind power producing countries," *Renewable and Sustainable Energy Reviews*, vol. 19, pp. 348-359, 2013.

[15] D., Wemans, J., Lima, J., Malico, I., Carvalho, "Photovoltaic energy mini generation: Future perspectives for Portugal," *Energy Policy*, vol. 39, pp. 5465-5473, 2011.

[16] European Union EU, "Directive 2009/28/EC of the European Parliament and of the Council of 20 April on the Promotion of the use of energy from renewable sources and amending," 2009.

[17] (2014, December 1) photovoltaic barometer. [Online]. http://www.energies-renouvelables.org/

[18] (2014, December) International Energy Acengy. [Online]. www.ieawind.org

[19] B., Spanhoff, "Current status and future prospects of hydropower in saxony (Germany) compared to trends in Germany, the European Union and World," *Renewable and Sustainable Energy Reviews*, vol. 20, pp. 518-525, 2014.

[20] C., Meiss, J., Mueller, B., Hlusiak, M., Breyer, C., Kastner, M., Twelle, J., Moeller, "transforming the electricity generation of the Berlin-Brandenburg region, Germany," *Renewable Energy*, vol. 72, pp. 39-50, 2014.

[21] (2010, December) BGerman Govenment's energy concept - long term strategy for future energy supply. [Online]. https://www.bmu.de/files/english/pdf/application/pdf/energiekonzept_bundesregierung_en.pdf

[22] (2014, December 3) Annual_Statistics_2013. [Online]. http://www.ewea.org/

[23] A.M., Karteris, M.M. Papadopoulos, "An assessment of the Greek inventives scheme for photovoltaics," *Energy Policy*, vol. 37, pp. 1945-1952, 2009.

[24] A., Koroneos, C., Wangensteen, I., Roinioti, "Modeling the Greek energy system: Scenarios of clean energy use and their implications," *Energy Policy*, vol. 50, pp. 711-722, 2012.

[25] J., Kunz, F., Hirschhausen, C.V., Egerer, "Development scenarios for the North and Baltic Seas Grid- A welfare economic analysis," *Utility Policy*, vol. 27, pp. 123-134, 2013.

[26] G., Sidiropoulos, C., Pentaliotis, A., Tsilingiridis, "Reduction of air pollutant emissions using renewable energy sources for power generation in Cyprus," *Renewable Energy*, vol. 36, pp. 3292-3296, 2011.

[27] (2014, May) Cyprus has moved closer to reaching European Union's renewable energy target by 2020. [Online]. www.worldofwindenergy.com

[28] Electricity Authority of Cyprus. (2014, December 10) Electricity Authority of Cyprus. [Online]. www.eac.com.cy

[29] M.T Arsalan, "METHODOLOGY TO SIZE LARGE SCALE SOLAR PV INSTALLATIONS FOR INSTITUTIONS WITH UNIDIRECTIONAL METERING," Cyprus, 2014.

[30] K., Millar, D.L., Trapani, "Proposing offshore photovoltaic technology to the energy mix of the Maltese Islands," *Energy Conversion Management*, vol. 67, pp. 18-26, 2013.

[31] (2014, December 5) Northern Cyprus Cyprus Electricity Authority. [Online]. http://www.kibtek.com/Santrallar

[32] J.A. & Beckman, W.A. Duffie, *Solar Engineering of Thermal Process*., 2006.

[33] D. K. Baker, "SEES 510 Spring 2012 Class Notes," Cyprus, 2012.

[34] S., Claywell, R., & Muneer, T. Younes, "Quality control of solar radiation data: Present status and porposed new approaches," *Energy*, vol. 30, pp. 1533-1549.

[35] I. Moradi, "Quality control of global solar radiation using sunshine duration hours," *Energy*, vol. 34, pp. 1-6.

[36] A.M.K. El-Ghonemy, "Photovoltaic Solar Energy: Review," *International Journal of Scientific & Engineering Research*, vol. 3, no. 11, November 2012.

[37] (2014, December) Engineering Library. [Online]. http://www.engineering.com/SustainableEngineering/RenewableEnergyEngineering/SolarEnergyEngineering/Photovoltaics/tabid/3890/Default.aspx

[38] (2014, November) National Aeronautics and Space Administration (NASA). [Online]. http://science.nasa.gov/science-news/science-at-nasa/2002/solarcells/

[39] T and Castaner, L Markvart, "Practical Handbook of Photovoltaics, Fundamentals and Applications," in *Practical Handbook of Photovoltaics, Fundamentals and Applications*.: Elsevier, 2013.

[40] Ci-Siang Tu, and Yi-Jie Su Huan-Liang Tsai, "Development of Generalized Photovoltaic Model Using MATLAB/SIMULINK‖," in *Proceedings of the World Congress on Engineering and Computer Science*, San Francisco-USA, 22-24 October 2008.

[41] Makarand Lokhande, Mukesh Patel inal Kachhiya, "MATLAB/Simulink Model of Solar PV Module and MPPT Algorithm‖," in *National Conference on Recent Trends in Engineering & Technology*, Gujarat, India, 2011.

[42] L. Castaner and S. Silvestre, *Modeling Photovoltaic Systems using Pspice*. England: John Wiley &Sons, 2002.

[43] D. Sera and R. & Rodriguez, P. Teodorescu, "PV panel model based on datasheet values," in *IEEE International Symposium on Industrial Electronics*, Spain, June 2007.

[44] W. De Soto and S.A. & Beckman, W.A. Klein, "Improvement and validation of a model for photovoltaic array performance," *Solar Energy*, vol. 80, no. 1, pp. 78-88, June 2006.

[45] A.N. Celik and N. Acikgoz, "Modeling and experimental verification of the operating current of mono-crystalline photovoltaic modules using four- and five-parameter models," *Applied Energy*, vol. 84, no. 1, pp. 1-15, 2007.

[46] R. henni, M. Makhlouf, and T. & Bouzid, A. Kerbache, "A detailed modeling method for photovoltaic cells," *Energy*, vol. 32, no. 9, pp. 1724-1730, 2007.

[47] Geoff R. Walker, "Evaluating MPPT Converter Topologies Using a MATLAB PV Model," in *Australasian Universities Power Engineering Conference*, Brisbane, Australia, 2000.

[48] N. Pandiarajan and Ranganath Muthu, "Mathematical Modeling of Photovoltaic Module with Simulink," in *International Conference on Electrical Energy Systems*, 3-5 January 2011.

[49] B., Gholamreza, F., Rahmani, K. Taherbaneh. Evaluation the accuracy of one-diode and two diode models for a solar panel based open-air climate masurements. [Online]. www.intechopen.com

[50] K., Lokhande, M., Patel, M. Kachhiya, "MATLAB/Simulink model of solar PV module and MPPT algorithm," in *National Conference on Recent Trends in Engineering and Technology*, Engineering College, V.V.Nagar,Gujarat-, 13-14 May

2011.

[51] M. Ragheb. (2014) Wind Energy Conversion Theory: Betz's Equation.

[52] M., & Ragreb, A. M. Ragreb, "Wind Turbine Theory - Betz Equation and Optimal Rotor Tip Speed Ratio," 2014.

[53] A., Diez, D., Molina, C., & Gil, M. Water Santos, "Water consumption in solar parabolic trough plants: review and analysis of the southern Spain Case," *Renewable and Sustainable Energy Reviews*, vol. 34, pp. 565-577.

[54] S., ULUPINAR, Y., DEMIRCAN, Y., ALAN, I., AKYUREK, Z., BOSTAN, Z.A. SENSOY, "Modeling Solar Energy Potential In Turkey," Ankara, Turkey, 2010.

[55] M. Fahrioğlu, "CSP work shop notes," 2013.

[56] J.P Sayler, "Vestas V66 General Specifications," 2007.

[57] "Vestas V27 Wind Turbine Specifications," UK, 2014.

[58] (2014, December) Cyprus has moved closer to reaching the European Union's renewable energy target by 2020. [Online]. www.worldofwindenergy.com

[59] (2014, December) Electricity Authority of Cyprus. [Online]. www.eac.com.cy

[60] P.E. Morthorst. Cost and Prices Facts. [Online]. www.ewea.org

[61] C., Assiakopoulos, V., Tymvios, F., Theophilou, K., & Asimakopoulos, D. acovides, "Solar global UV(280-380nm) radiation and its relationship with solar global radiation measured on the island of Cyprus," *Energy*, vol. 31, pp. 2728-2738, 2006.

[62] F., & Midner, R. Martini, "The Serhatköy Photovoltaic Power plant and the future of Renewable Energy on the Turkish Republic of Northern Cyprus," 2013.

[63] (2014, December 3) International Energy Agency. [Online]. http://www.iea.org/statistics/topics/Electricity/

[64] (2014, December) EPIA_Global_Market_Outlook_for_Photovoltaics_2014-2018_-_Medium_Res. [Online]. http://www.epia.org/

[65] (2014, December) National Renewable Energy Laboratory. [Online]. http://www.nrel.gov/

[66] (2014, May 25) Wikipedia. [Online]. http://en.wikipedia.org/wiki/File:Betz_tube.jpg

[67] (2014, December 4) Windpower. [Online]. http://www.thewindpower.net/actor_content_en.php?id_type=5

APPENDIX A

COMPARISON OF METU NCC AND SERHATKÖY SOLAR RESOURCE DATA

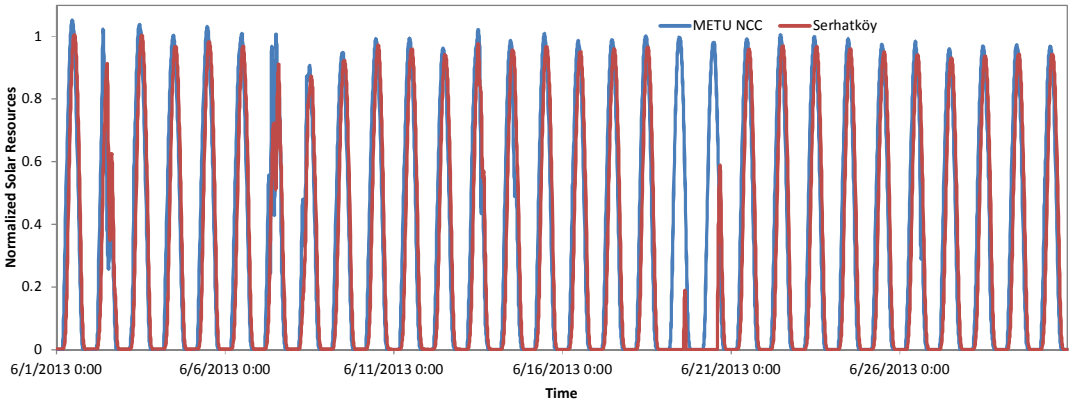

Figure A 1 :Comparison between Normalized METU NCC and Serhatköy Solar Resource Data for June 2013 [**29**]

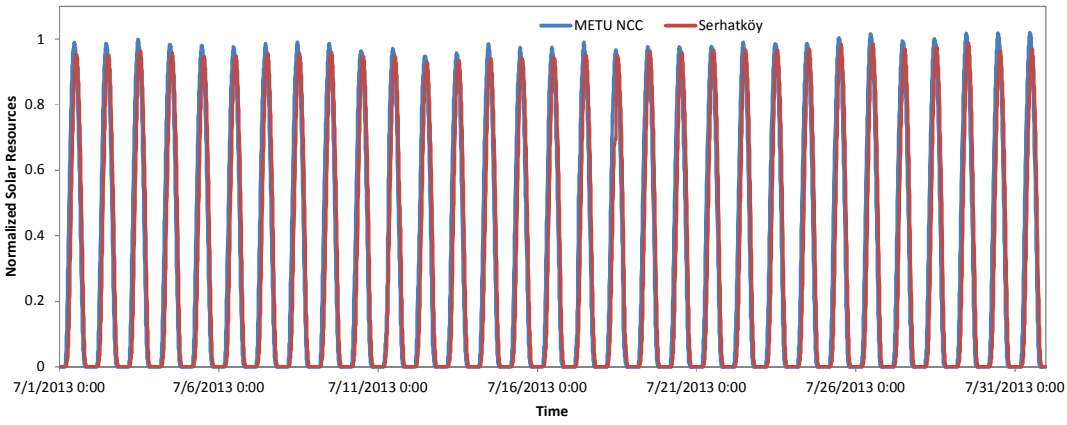

Figure A 2 :Comparison between Normalized METU NCC and Serhatköy Solar Resource Data for July 2013 [**29**]

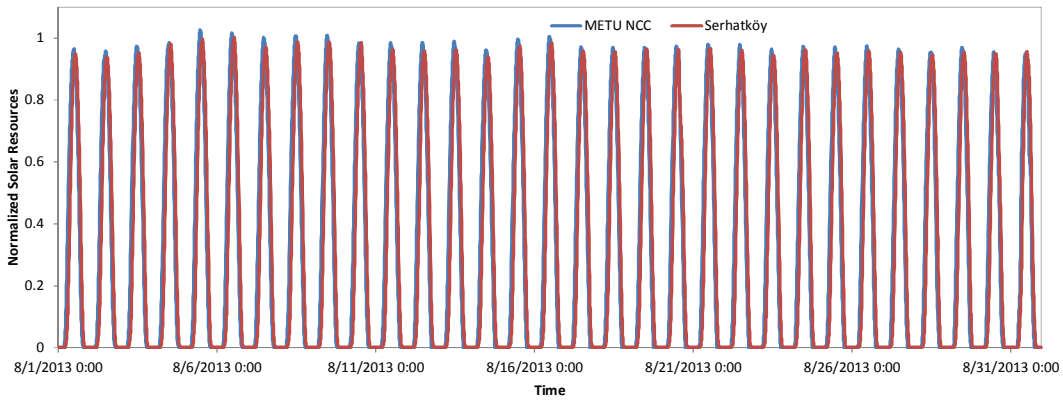

Figure A 3 :Comparison between Normalized METU NCC and Serhatköy Solar Resource Data for August 2013 [**29**]

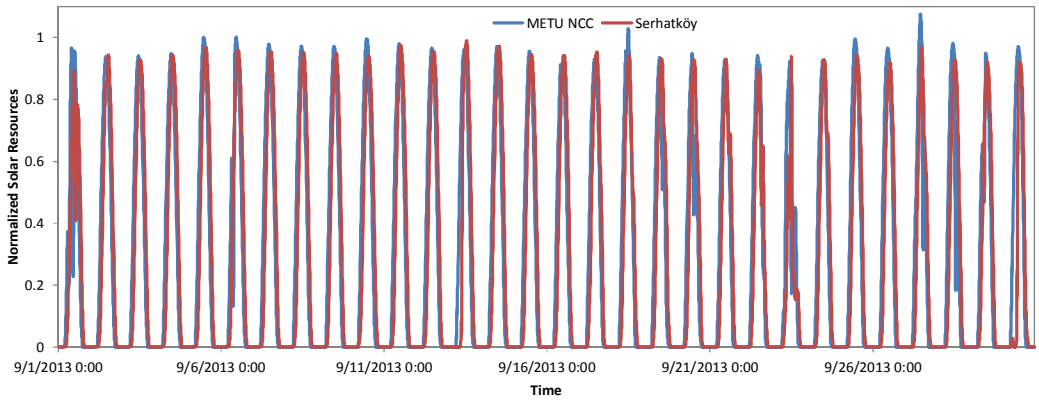

Figure A 4 :Comparison between Normalized METU NCC and Serhatköy Solar Resource Data for September 2013 [**29**]

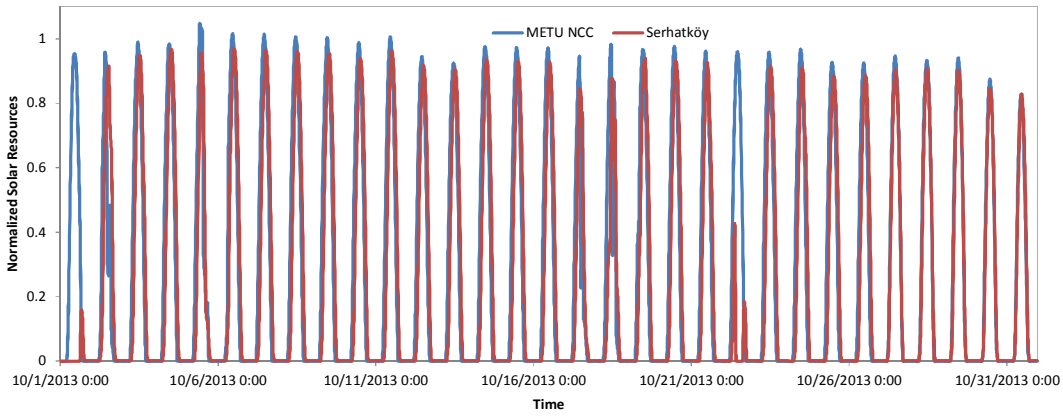

Figure A 5 :Comparison between Normalized METU NCC and Serhatköy Solar Resource Data for October 2013 [**29**]

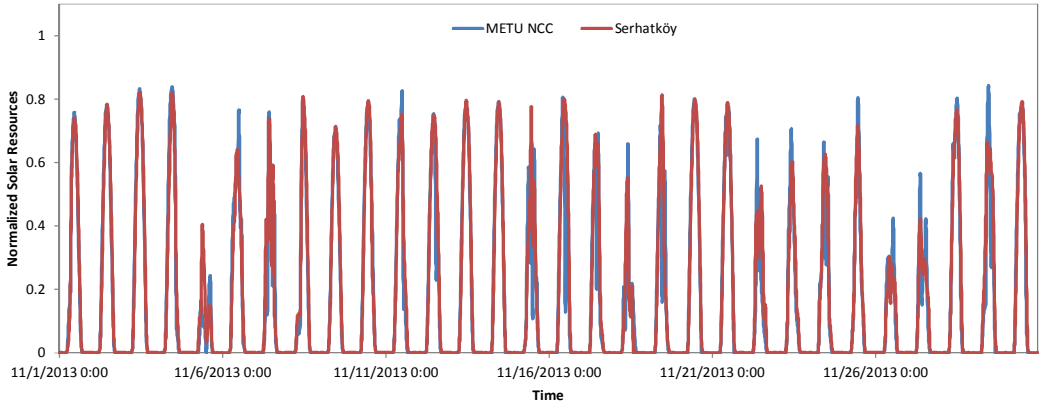

Figure A 6 :Comparison between Normalized METU NCC and Serhatköy Solar Resource Data for November 2013 [**29**]

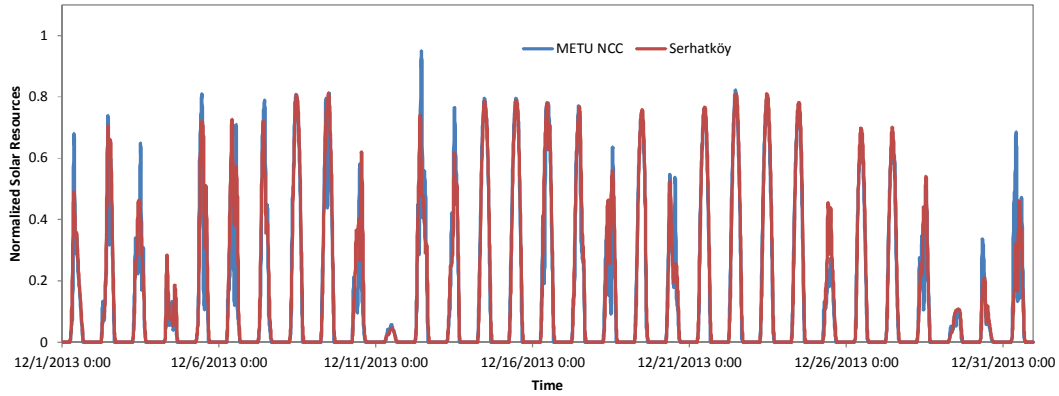

Figure A 7 :Comparison between Normalized METU NCC and Serhatköy Solar Resource Data for December 2013 [**29**]

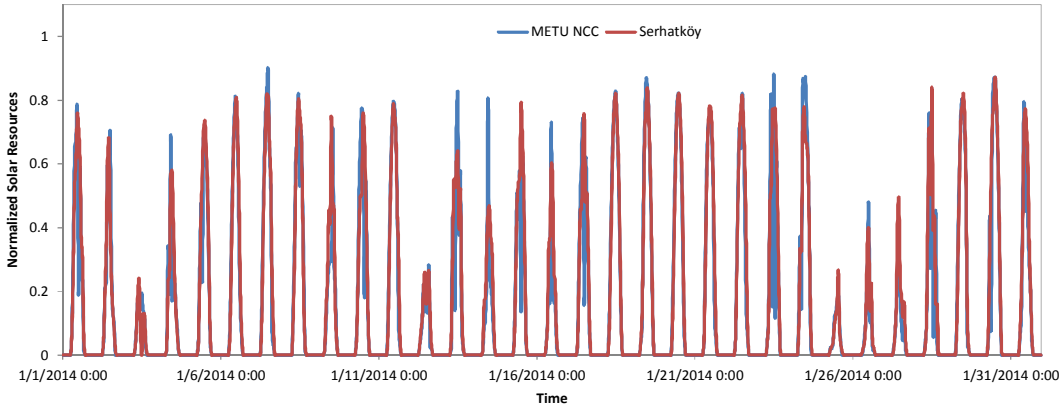

Figure A 8 :Comparison between Normalized METU NCC and Serhatköy Solar Resource Data for January 2014 [**29**]

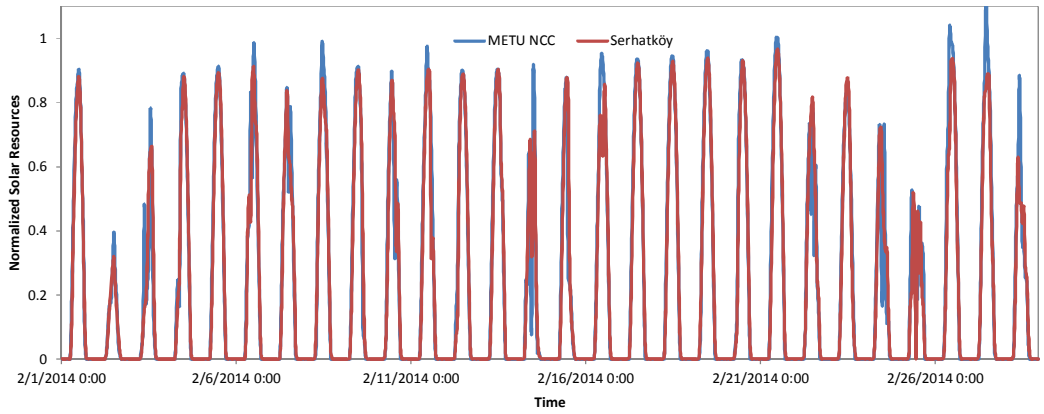

Figure A 9 :Comparison between Normalized METU NCC and Serhatköy Solar Resource Data for February 2014 [**29**]

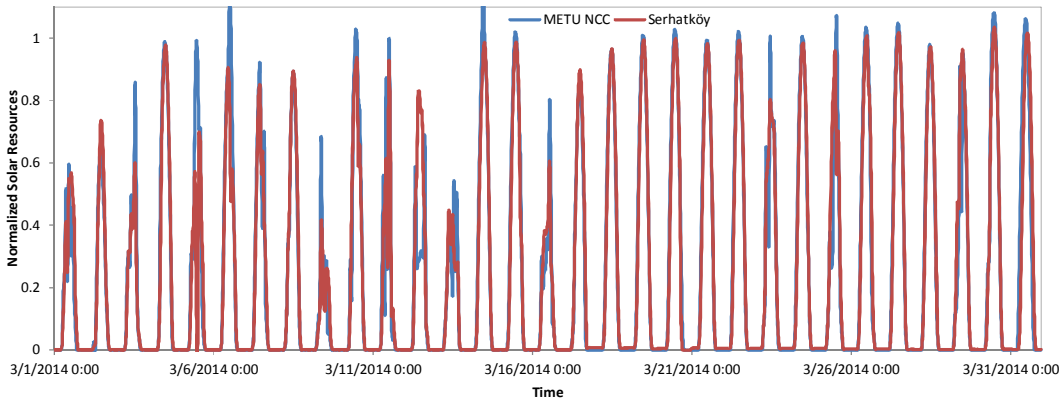

Figure A 10 :Comparison between Normalized METU NCC and Serhatköy Solar Resource Data for March 2014 [**29**]

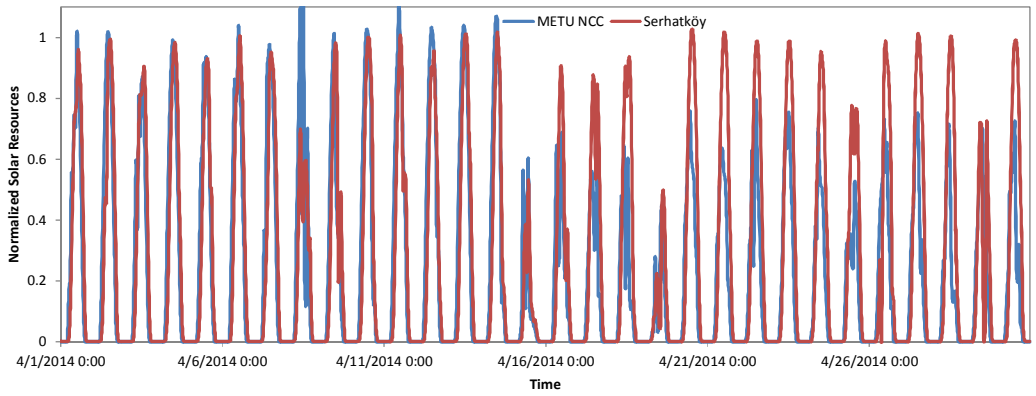

Figure A 11 :Comparison between Normalized METU NCC and Serhatköy Solar Resource Data for April 2014 [**29**]

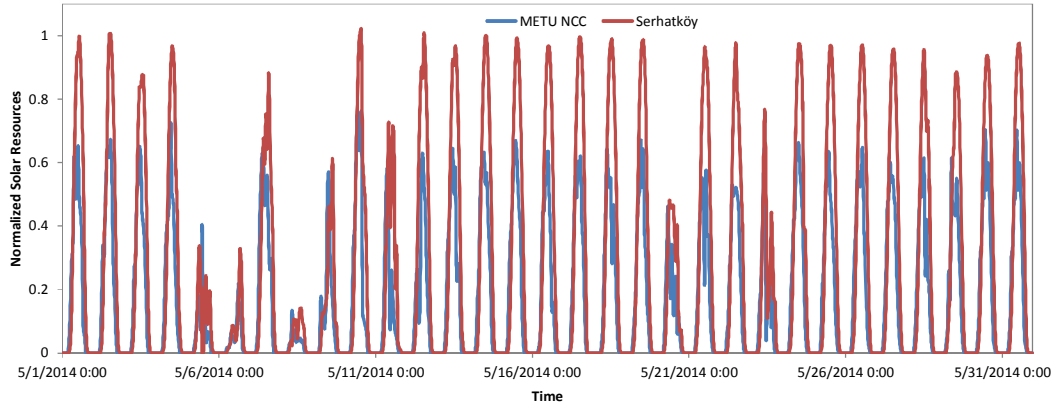

Figure A 12 :Comparison between Normalized METU NCC and Serhatköy Solar Resource Data for May 2014 [**29**]

Table A 1 Comparison of annual solar resources between METU NCC and Serhatköy [**29**]

Month	METU NCC Wh m^{-2}	Serhatköy Wh m^{-2}	Difference %
Jun-13	234,869	205,929	-14.05%
Jul-13	241,000	227,281	-6.04%
Aug-13	230,722	221,579	-4.13%
Sep-13	202,009	193,366	-4.47%
Oct-13	200,283	178,856	-11.98%
Nov-13	111,438	116,589	4.42%
Dec-13	99,227	105,537	5.98%
Jan-14	107,522	116,278	7.53%
Feb-14	147,778	142,912	-3.40%
Mar-14	180,293	178,015	-1.28%
Apr-14	163,187	191,034	14.58%
May-14	122,837	194,126	36.72%
Annual	2,041,168	2,071,502	1.46%